

PP-graphics with a nilpotent elliptic singularity in quadratic systems and Hilbert's 16th problem

Christiane Rousseau*

Department of Mathematics and Statistics
University of Montreal, Montreal, Quebec, Canada, H3C 3J7

Huaiping Zhu†

Department of Mathematics and Statistics
York University, Toronto, Ontario, Canada, M3J 1P3

Abstract

This paper is part of the program launched in [4] to prove the finiteness part of Hilbert's 16th problem for quadratic system, which consists in proving that 121 graphics have finite cyclicity among quadratic systems. We show that any pp-graphic through a multiplicity 3 nilpotent singularity of elliptic type which does not surround a center has finite cyclicity. Such graphics may have additional saddles and/or saddle-nodes. Altogether we show the finite cyclicity of 15 graphics of [4]. In particular we prove the finite cyclicity of a pp-graphic with an elliptic nilpotent singular point together with a hyperbolic saddle with hyperbolicity $\neq 1$ which appears in generic 3-parameter families of vector fields and hence belongs to the zoo of Kotova-Stanzo [11].

1 Introduction

This paper is part of a large attack on the finiteness part of Hilbert's 16th problem for quadratic fields which consists in proving the existence of a uniform bound for the

*Supported by NSERC and FCAR in Canada, E-mail: rousseac@dms.umontreal.ca

†Partially supported by an NSERC postdoctoral fellowship and Startup fund of York University, E-mail: huaiping@mathstat.yorku.ca

number of limit cycles of a quadratic vector field

$$P(x, y) \frac{\partial}{\partial x} + Q(x, y) \frac{\partial}{\partial y}. \quad (1.1)$$

In [4], the following theorem is proved:

Theorem 1.1. *There exists a uniform bound for the number of limit cycles of a quadratic vector field if and only if all limit periodic sets surrounding the origin inside the family*

$$\begin{cases} \dot{x} = \lambda x - \mu y + a_1 x^2 + a_2 xy + a_3 y^2 \\ \dot{y} = \mu x + \lambda y + b_1 x^2 + b_2 xy + b_3 y^2 \end{cases} \quad (1.2)$$

have finite cyclicity inside (1.2).

The complete list of 121 graphics was also given. The program is progressing well and several papers have permitted to prove the finite cyclicity of nearly all elementary graphics ([1], [2], and [5]). The paper of Dumortier, Roussarie and Sotomayor [7] is the first study of a graphic with a nilpotent point. The ideas have been refined in Zhu and Rousseau [15] and extended and have permitted to prove the finite cyclicity of several graphics of codimension 3 or 4 passing through a nilpotent point of saddle or elliptic type. The finite cyclicity theorems usually have genericity conditions on the regular transition map along the graphic.

In this paper we apply the theorems and/or methods of [15] to all the pp-graphics through a nilpotent singularity of elliptic type appearing in the list of [4]. In some cases the finite cyclicity follows from a verification of the genericity conditions inside quadratic systems while in others the proofs of [15] must be adapted to graphics which may have up to three additional elementary singular points (one or two hyperbolic saddles and/or one saddle-node). The proofs given in [15] are very complete. The applications to quadratic systems require long calculations and checking of details. In the present paper we have tried to keep the proofs to a minimum as long as they require no new ideas and are copied on “classical” proofs of finite cyclicity for elementary graphics.

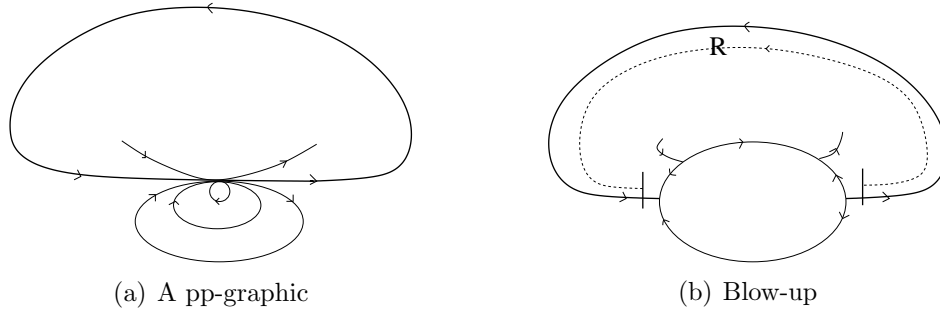


Figure 1: pp-graphics with a nilpotent elliptic point having finite cyclicity

From the results of [15], we will also be able to prove the finite cyclicity of several graphics in [4]: hp-graphics and hh-graphics with a nilpotent elliptic point and graphics through a nilpotent saddle. As the calculations are quite long and some are subtle, these will be treated in a forthcoming publication.

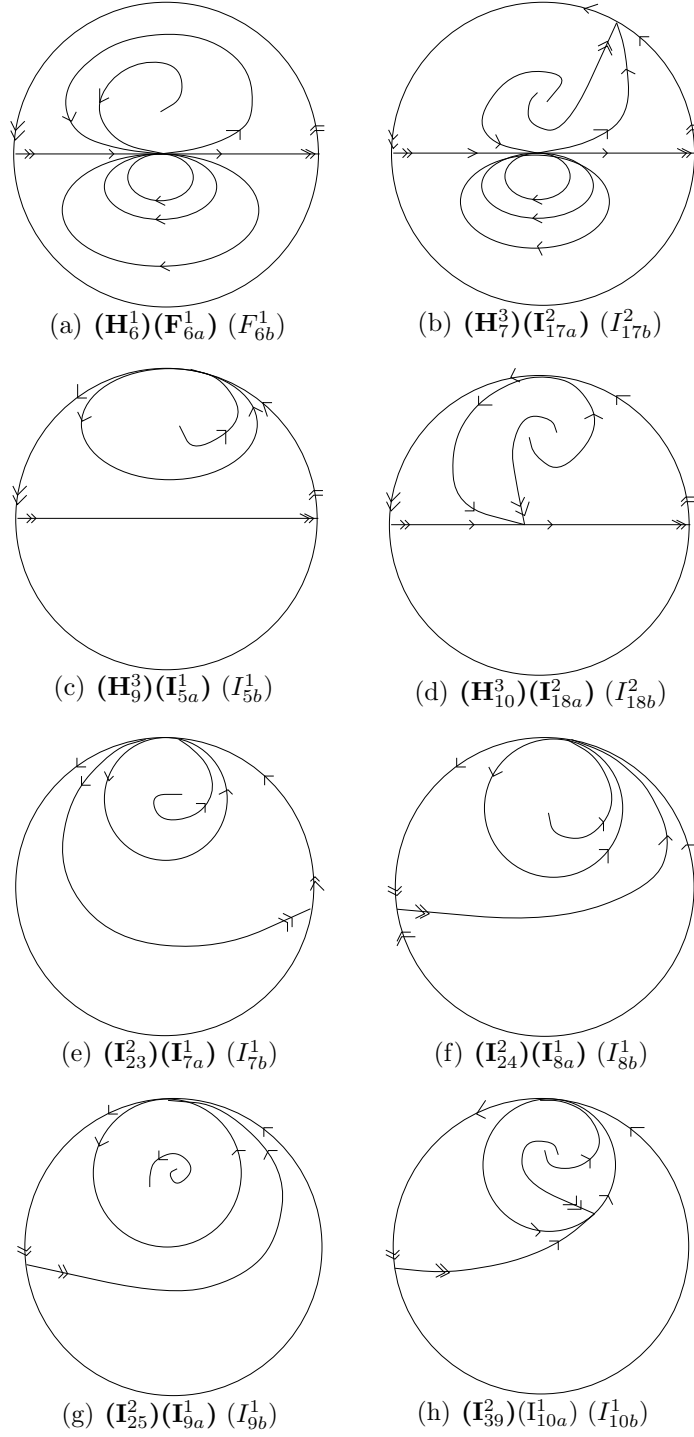


Figure 2: The 15 pp-graphics for which we prove finite cyclicity (the finite cyclicity of (I_{10a}^1) is proved in [3])

2 Preliminaries

2.1 General finite cyclicity theorems

The following theorem is proved in [15]:

Theorem 2.1. *A pp-graphic with a triple nilpotent elliptic point (Epp) of any codimension with 2 parabolic and 2 hyperbolic sectors (Fig. 1) has cyclicity $\leq n$ ($\text{Cycl}(\text{Epp}) \leq n$) if the regular transition map R calculated using normalizing coordinates has its n -th derivative non-vanishing.*

To check the hypothesis, we do not need to unfold the family. A simple blow-up $(x, y) = (r\bar{x}, r^2\bar{y})$ will be sufficient. As shown in Fig. 1b, we will take normalizing coordinates near the two nodes on the blow-up circle. The map R is defined on sections parallel to the coordinate axes defined in these charts.

2.2 Statement of the result

Theorem 2.2. *All the 16 pp-graphics listed in Fig. 2 have finite cyclicity.*

Remark 2.3. *For the none pp-graphics listed in Fig.2:*

1. Graphics (F_{6b}^1) , (I_{5b}^1) , (I_{7b}^1) and (I_{8b}^1) have finite cyclicity by [15].
2. Graphics (I_{17b}^1) and (I_{18b}^1) are still open.
3. Graphics (I_{9b}^1) and (I_{10b}^1) have finite cyclicity but the proof is not yet published.
4. The proof of the finite cyclicity of (I_{10a}^1) appears in [3].

2.3 Dulac map near a hyperbolic saddle in the plane

To prove the finite cyclicity results, we need the following statements about the Dulac maps near a hyperbolic saddle.

Definition 2.4.

1. A singular point is elementary if it has at least one nonzero eigenvalue. It is hyperbolic (resp. semi-hyperbolic) if the two eigenvalues are not on the imaginary axis (resp. exactly one eigenvalue is zero).
2. The hyperbolicity ratio at a hyperbolic saddle is the ratio $\sigma = -\frac{\lambda_1}{\lambda_2}$, where $\lambda_1 < 0 < \lambda_2$ are the two eigenvalues.

Let $(X_\lambda)_{\lambda \in \Lambda}$, be a C^∞ family of vector fields defined in the neighborhood of a hyperbolic saddle at the origin. We also assume that the coordinate axes are the invariant manifolds near the saddle point. By normal form theory, we can for any fixed $k \in \mathbb{N}$, up to C^k -equivalence write the family of vector fields X_λ into some explicit normal form (cf. [13], [10]). Let $\sigma(\lambda)$ be the hyperbolicity ratio of X_λ at the origin.

- If $\sigma(0)$ is irrational, then, $\forall k \in \mathbb{N}$, the family of vector fields X_λ is C^k -equivalent to

$$\begin{cases} \dot{x} &= x \\ \dot{y} &= -\sigma(\lambda)y \end{cases} \quad (2.1)$$

for λ in some neighborhood W of the origin in parameter space.

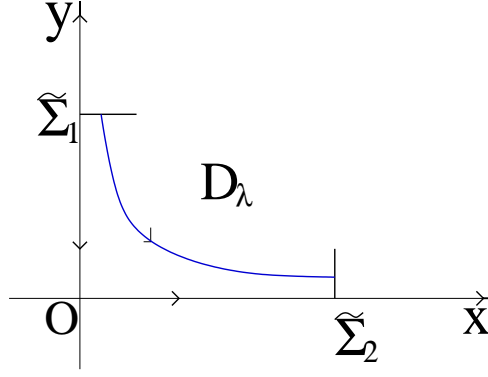


Figure 3: Dulac map near a hyperbolic saddle in the plane

- If $\sigma(0) = \frac{p}{q} \in \mathbb{Q}$, $(p, q) = 1$. Then $\forall k \in \mathbb{N}$, the family X_λ is C^k -equivalent to

$$\begin{cases} \dot{x} &= x \\ \dot{y} &= y \left[-\frac{p}{q} + \sum_{i=0}^{N(k)} \alpha_{i+1}(\lambda) (x^p y^q)^i \right]. \end{cases} \quad (2.2)$$

for λ in some neighborhood W of the origin in parameter space. In particular, $\alpha_1 = \sigma(0) - \sigma(\lambda)$.

Let $\tilde{\Sigma}_1 = \{y = y_0\}$ and $\tilde{\Sigma}_2 = \{x = x_0\}$ be two sections transverse to the vector field X_λ (Fig. 3), where $x_0, y_0 > 0$ constants. The flow of X_λ induces a Dulac map $D_\lambda(\cdot, \lambda)$:

$$D_\lambda : \tilde{\Sigma}_1 \longrightarrow \tilde{\Sigma}_2$$

for all $\lambda \in W$.

The Dulac map is C^∞ for $x > 0$. The following theorem of Mourtada ([12]) describes its behavior near $x = 0$.

Proposition 2.5. (Mourtada) *The Dulac map D_λ can be written as*

$$D_\lambda(x) = x^{\sigma(\lambda)} [c(\lambda) + \psi(x, \lambda)] \quad (2.3)$$

where $c(\lambda) = \frac{y_0}{x_0^{\sigma(\lambda)}}$, $\psi(x, \lambda)$ is C^∞ for $(x, \lambda) \in (0, x_0] \times W$. Furthermore, ψ satisfies the following property (I_0^∞) :

$$(I_0^\infty) : \forall n \in \mathbb{N}, \lim_{x \rightarrow 0} x^n \frac{\partial^n \psi}{\partial x^n}(x, \lambda) = 0 \quad \text{uniformly for } \lambda \in W \quad (2.4)$$

where

1. if $\sigma(0) \notin \mathbb{Q}$, then $\psi \equiv 0$;
2. if $\sigma(0) = \frac{p}{q}$, then we have the more precise expression (see [1]).

Let

$$\omega(x, \alpha_1) = \begin{cases} \frac{x^{-\alpha_1-1}}{\alpha_1} & \text{if } \alpha_1 \neq 0 \\ -\ln x & \text{if } \alpha_1 = 0. \end{cases} \quad (2.5)$$

be the Ecalle-Roussarie compensator of the vector field X_λ where $\alpha_1(\lambda) = \sigma(0) - \sigma(\lambda)$. Then

$$D_\lambda(x) = x^{\sigma(\lambda)} \left(1 + \sum_{1 \leq j \leq i \leq K(k)} \beta_{ij} x^{ip} \omega^j + \bar{\psi}_k(x, \lambda) \right) \quad (2.6)$$

where $\bar{\psi}_k(x, \lambda)$ is k -flat.

Consequently the map $\psi(x, \lambda)$ in (2.3) has the form $\psi(x, \lambda) = o(x^\eta)$ for all $\eta < 1$.

Proposition 2.6. *The C^k -normal form for a family unfolding a saddle-node is*

$$\begin{cases} \dot{x} &= x^2 - \varepsilon \\ \dot{y} &= \pm y(1 + ax). \end{cases} \quad (2.7)$$

The transition Dulac map from $x = -x_0$ to $x = x_0$ has the form

$$y \mapsto m(\varepsilon)y \quad (2.8)$$

where $\lim_{\varepsilon \rightarrow 0} m(\varepsilon) = +\infty$ (resp. $\lim_{\varepsilon \rightarrow 0} m(\varepsilon) = 0$) for a repelling (resp attracting) saddle-node.

The next proposition developed in [2] and [15] will be used to calculate the first and second order derivatives of a regular transition map of a vector field.

Proposition 2.7. *Consider the regular transition map R for a vector field*

$$\begin{aligned} \dot{x} &= P(x, y) \\ \dot{y} &= Q(x, y) \end{aligned} \quad (2.9)$$

between two arcs without contact $\Sigma_1 = \{y = y_1\}$ and $\Sigma_2 = \{y = y_2\}$. The formulas are simpler if we add the following hypotheses

- $P(0, y) \equiv 0$, so the transition is along the axis $x = 0$;
- $Q(0, y) \neq 0$ for $y \in (y_1, y_2)$.

Then

$$R'(0) = \exp \left(\int_{y_1}^{y_2} \frac{P'_x}{Q}(0, y) dy \right), \quad (2.10)$$

$$R''(0) = R'(0) \int_{y_1}^{y_2} \left(\frac{P''_x}{Q}(0, y) - 2 \frac{P'_x Q'_x}{Q^2}(0, y) \right) \exp \left(\int_{y_1}^y \frac{P'_x}{Q}(0, z) dz \right) dy. \quad (2.11)$$

2.4 Normal forms near nilpotent singularities of multiplicity 3

We present two normal forms: the classical one of Dumortier and Roussarie [6] which allows the reader to understand our results with no translation needed and a second one which has been proved to be particularly convenient in [15] and which is well adapted to applications to quadratic systems since its principal part is quadratic instead of cubic.

A family containing a triple nilpotent singularity of elliptic type with two parabolic sectors can be written as ([6])

$$\begin{cases} \dot{x} &= y \\ \dot{y} &= -x^3 + \lambda_2 x + \lambda_1 + y(\lambda_3 + bx + \varepsilon_2 x^2 + x^3 h(x, \lambda)) + y^2 Q(x, y, \lambda) \end{cases} \quad (2.12)$$

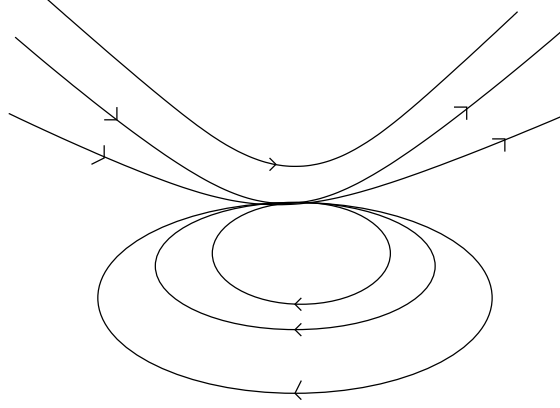


Figure 4: An elliptic nilpotent point

where $b > 2\sqrt{2}$ (Fig. 4), $\lambda = (\lambda_1, \lambda_2, \lambda_3, \hat{\lambda})$ are the parameters, $Q(x, y, \lambda)$ is C^∞ in (x, y, λ) and of arbitrarily high order in (x, y, λ) .

For the purpose of studying the passages in the neighborhood of the nilpotent singularity, in [15] we developed a new normal form for the unfolding of the nilpotent singularity of the saddle and elliptic type. For the elliptic case, we have

Theorem 2.8. *The family (2.12) is C^∞ -equivalent to*

$$\begin{cases} \dot{X} &= Y + \mu_2 + aX^2 \\ \dot{Y} &= \mu_1 + Y(\mu_3 + X + \bar{\varepsilon}_2 X^2 + X^3 h_1(X, \mu)) + X^4 h_2(X, \mu) + Y^2 Q(X, Y, \mu) \end{cases} \quad (2.13)$$

where $a \in (0, \frac{1}{2})$, $\bar{\varepsilon}_2 = a\varepsilon_2$, and $\mu = (\mu_1, \mu_2, \mu_3, \hat{\mu})$ is the parameter, $h_1(X, \mu)$, $h_2(X, \mu) = \bar{\varepsilon}_2 a + O(\mu) + O(X)$ and $Q(X, Y, \mu)$ are C^∞ and $Q(X, Y, \mu)$ is of arbitrary high order in (X, Y, μ) .

If $a = \frac{1}{2}$, the unfolding is of codimension 4, type 1, which corresponds to the case $b = 2\sqrt{2}$ (the two characteristic trajectories coalesce into one).

Remark 2.9. *If $\varepsilon_2 = 0$, the 3-parameter unfolding (2.13) is not universal. In this case, the codimension of the nilpotent singularity is at least 4.*

2.5 Quadratic systems with a nilpotent singular point in the finite plane

Theorem 2.10. *A quadratic system with a nilpotent singular point of multiplicity 3 at the origin and an anti-saddle in the upper half-plane is linearly equivalent to*

$$\begin{cases} \dot{x} &= y + ax^2 + cxy - y^2 \\ \dot{y} &= xy. \end{cases} \quad (2.14)$$

where $a \neq 0$ and $c \in \mathbb{R}$.

Proof. By Jordan normal form theorem, we can write the quadratic system with a triple nilpotent singular point of saddle or elliptic type at the origin in the form

$$\begin{cases} \dot{x}_1 &= y_1 + a_1 x_1^2 + b_1 x_1 y_1 + c_1 y_1^2 \\ \dot{y}_1 &= e_1 x_1 y_1 + f_1 y_1^2 \end{cases} \quad (2.15)$$

where $a_1 e_1 \neq 0$.

By a linear transformation

$$\begin{cases} x_1 &= \frac{1}{e_1} x_2 - \frac{f_1}{e_1^2} y_2 \\ y_1 &= \frac{1}{e_1} y_2 \end{cases}$$

system (2.15) is equivalent to

$$\begin{cases} \dot{x}_2 &= y_2 + a_2 x_2^2 + b_2 x_2 y_2 + c_2 y_2^2 \\ \dot{y}_2 &= x_2 y_2. \end{cases} \quad (2.16)$$

Adding an additional singular point on the y -axis, we should have $c_2 \neq 0$. This singular point is an anti-saddle if $c_2 < 0$. By rescaling we get (2.14). It follows from Theorem 2.10 that for $a \in (0, \frac{1}{2})$, the nilpotent point at the origin is elliptic. \square

One can verify that for (2.14) with $a \in (0, \frac{1}{2})$, if $0 < c < 2\sqrt{1-a}$, we have (H_6^1) , if $c = 2\sqrt{1-a}$, we have (H_7^3) . We will use (2.14) to prove the finite cyclicity for (H_6^1) .

2.6 Quadratic systems with a nilpotent singular point at infinity

Theorem 2.11. *A quadratic system with a triple singularity point of elliptic type at infinity and a finite singular point of focus or center type can be brought to the form*

$$\begin{cases} \dot{x} &= \delta x - y + Ax^2 \\ \dot{y} &= x + \gamma y + xy \end{cases} \quad (2.17)$$

with $A < 1$. For the graphics of Fig.2(c)-(h) we will have $\frac{1}{2} < A < 1$. Moreover,

1. The system has an invariant line $y = -1$ if $\gamma = 0$.
2. The value of “a” in the corresponding normal form (2.13) is $a = 1 - A$. For the graphics of Fig.2(c)-(h), $0 < a < \frac{1}{2}$.

Proof. We can suppose that the nilpotent singular point at infinity is located on the y -axis and the other singular point at infinity on the x -axis. Then the system can be brought to the form

$$\begin{cases} \dot{x} &= \delta_{10}x + \delta_{01}y + \delta_{20}x^2 + \delta_{11}xy \\ \dot{y} &= \gamma_{10}x + \gamma_{01}y + \gamma_{11}xy + \gamma_{02}y^2. \end{cases} \quad (2.18)$$

For the finite singular point to be an anti-saddle, we should have $\delta_{10}\gamma_{01} - \delta_{01}\gamma_{10} > 0$.

Localizing the system (2.18) at the singular point at infinity on y -axis by $v = \frac{x}{y}$, $z = \frac{1}{y}$, we then have

$$\begin{cases} \dot{v} &= (\delta_{11} - \gamma_{02})v + \delta_{01}z + (\delta_{20} - \gamma_{11})v^2 + (\delta_{10} - \gamma_{01})vz - \gamma_{10}v^2z \\ \dot{z} &= z(-\gamma_{02} - \gamma_{01}z - \gamma_{11}v - \gamma_{10}vz) \end{cases} \quad (2.19)$$

The singular point $(0, 0)$ of system (2.19) is nilpotent, we should have $\delta_{11} = \gamma_{02} = 0$. The point is triple if $\gamma_{11}(\delta_{20} - \gamma_{11}) \neq 0$. By a rescaling and still using the original coordinates (x, y) , we obtain the system (2.17)

Note that to bring (2.19) to the form (2.14), we take $X = -v$, $Y = z$. \square

For system (2.17) with $A \in (\frac{1}{2}, 1)$ and $\gamma = 0$, if $0 < \delta < 2\sqrt{A}$, we have (H_9^3) , if $\delta = 2\sqrt{A}$, we have (H_{10}^3) . To make the calculation easier, we will use an equivalent for of (2.17) to prove the finite cyclicity of (H_{10}^3) .

In the following discussions, we will use \mathbb{P} to denote the intervals of the parameters a and A in each case. \mathbb{P} is defined in Tab.1.

	in the finite plane	at infinity
Elliptic type	$a \in (0, \frac{1}{2})$	$A \in (\frac{1}{2}, 1)$

Table 1: The definition of the interval \mathbb{P} in each case

2.7 Blow-up of the family (normal form)

We are interested in the family for $a \in \mathbb{P}$ where a can depend on parameters and (x, y, μ) in a neighborhood $U \times \Lambda$ of $(0, 0, 0)$. Taking Λ as a sphere, we make the change of parameters

$$\begin{cases} \mu_1 &= \nu^3 \bar{\mu}_1 \\ \mu_2 &= \nu^2 \bar{\mu}_2 \\ \mu_3 &= \nu \bar{\mu}_3 \end{cases} \quad (2.20)$$

where $\bar{\mu} = (\bar{\mu}_1, \bar{\mu}_2, \bar{\mu}_3) \in \mathbb{S}^2$ and $\nu \in (0, \nu_0)$. Adding to the system (2.13) the equation $\dot{\nu} = 0$, we have

$$\begin{cases} \dot{x} &= y + \nu^2 \bar{\mu}_2 + ax^2 \\ \dot{y} &= \nu^3 \bar{\mu}_1 + y \left[\nu \bar{\mu}_3 + x + \varepsilon_2 x^2 + x^3 h_1(x, \nu \bar{\mu}) \right] \\ &\quad + x^4 h_2(x, \nu \bar{\mu}) + y^2 Q(x, y, \nu \bar{\mu}) \\ \dot{\nu} &= 0. \end{cases} \quad (2.21)$$

We then make the weighted blow-up

$$\begin{cases} x &= r\bar{x} \\ y &= r^2\bar{y} \\ \nu &= r\rho \end{cases} \quad (2.22)$$

where $r > 0$ and $(\bar{x}, \bar{y}, \rho) \in \mathbb{S}^2$.

Note that for each $\bar{\mu}$, the foliation given by $\{\nu = r\rho = \text{const}\}$ is preserved by $\overline{X}_{(a, \bar{\mu})}$:

- For $\{r\rho = \nu\}$ with $\nu > 0$, the leaf is a regular manifold of dimension 2.
- For $\{r\rho = 0\}$, we get a stratified set in the critical locus. As shown in Fig. 5, there are two strata of 2-dimensional manifolds:

- $\hat{F}_{\bar{\mu}} \cong S^1 \times R^+$ the blow-up of the fibre $\mu = 0$,
- $D_{\bar{\mu}} = \{\bar{x}^2 + \bar{y}^2 + \rho^2 = 1, \rho \geq 0\}$.

On $\hat{F}_{\bar{\mu}} = \{\rho = 0\}$, (2.22) is just the common blow-up of the nilpotent point:

$$\begin{cases} x &= r\bar{x} \\ y &= r^2\bar{y} \end{cases} \quad (2.23)$$

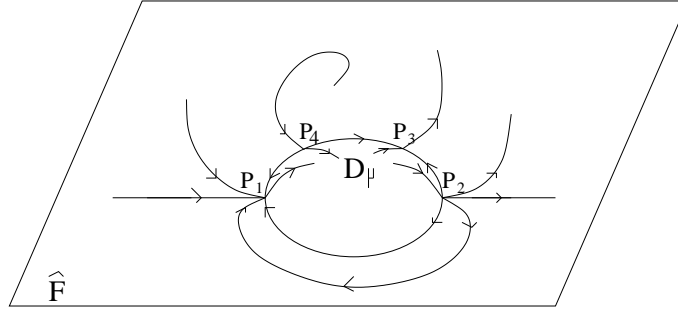


Figure 5: The stratified set $\{r\rho = 0\}$ in the blow-up

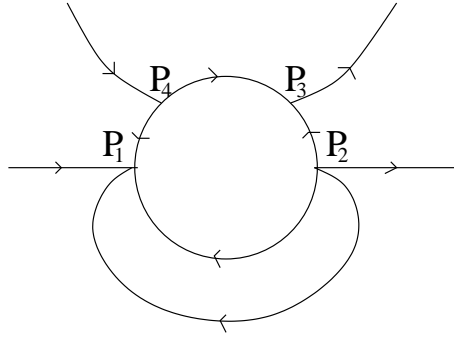


Figure 6: Common blow-up of the nilpotent singularity

and by the blow-up (2.23), we get a vector field with four singular points P_i ($i = 1, 2, 3, 4$). P_1 and P_2 are nodes, P_3 and P_4 are hyperbolic saddles (Fig. 6).

The four points P_i on the circle $x^2 + y^2 = 1$, $r = \rho = 0$ are studied in the charts $\bar{x} = \pm 1$, while the upper part of the sphere $r = 0$, $\rho > 0$ is studied in the chart $\rho = 1$.

In [15] we find the list of the phase portraits of (2.21) on this half sphere for the different values of $\bar{\mu}_i$. Together with the regular part of the graphics this gives us the list of limit periodic sets for which finite cyclicity must be proved. These appear in Table. 2.

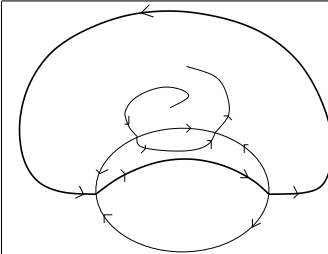
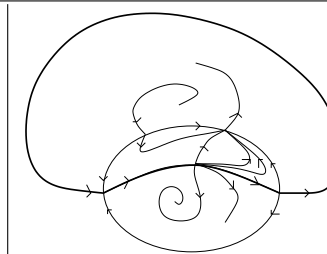
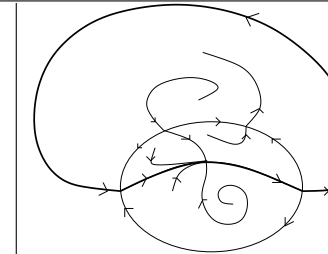
		
graphic Epp1	graphic Epp2	graphic Epp3

Table 2: Limit periodic sets of pp-type for the graphic with an elliptic point

2.8 Dulac maps near P_1 and P_2

To prove the finite cyclicity results in [15] we have proved results about the two different types of Dulac maps near the points P_1 (resp. P_2) and P_3 (resp. P_4). For the purpose of proving the finite cyclicity of pp-graphics, we only need the first type of Dulac maps near P_1 and P_2 .

Although after blow-up we deal with a 3-dimensional vector field, because of the invariant foliation, we can consider the Dulac maps to be 1-dimensional maps. The first type is similar to the passage near a saddle-node while the second is similar to the passage near a hyperbolic saddle.

The eigenvalues at P_1 and P_2 appear in Tab. 2.8. Due to the special form of the family, the vector fields at each point P_1 and P_2 are linear in r and ρ after dividing by a C^∞ positive function. We study P_1 . The study near P_2 is similar. Let

$$\sigma_1(a) = \frac{1-2a}{a}.$$

	r	ρ	y
P_1	$-a$	a	$-(1-2a)$
P_2	a	$-a$	$(1-2a)$

Table 3: The eigenvalues at P_1 and P_2

Near P_1 , the system is of the form

$$X_{(a,\bar{\mu})} \begin{cases} \dot{r} &= -r \\ \dot{\rho} &= \rho \\ \dot{\bar{y}} &= -\sigma_1(a)\bar{y} + f_{(a,\bar{\mu})}(r, \rho, \bar{y}) \end{cases} \quad (2.24)$$

where

$$\begin{aligned} & f_{(a,\bar{\mu})}(r, \rho, \bar{y}) \\ &= \sigma_1(a)\bar{y} + \frac{-(1-2a)\bar{y} + 2\bar{y}^2 + \bar{y}[\varepsilon_2 r + \bar{\mu}_3 \rho + 2\bar{\mu}_2 \rho^2 - r^2 h_1(r, r\rho, \bar{\mu})] + \bar{\mu}_1 \rho^3 + r\bar{h}_2(r, r\rho, \bar{\mu}) + \bar{y}^2 \bar{Q}_2(r, \rho, \bar{y}, \bar{\mu})}{a + \bar{y} + \bar{\mu}_2 \rho^2} \end{aligned} \quad (2.25)$$

and the parameters $(a, \mu) \in \mathbb{P} \times \mathbb{S}^2$.

Proposition 2.12. *Consider the family $X_{(a,\bar{\mu})}$ in the form of (2.24) with parameters $(a, \bar{\mu}) \in \mathbb{P} \times \mathbb{S}^2$. Then $\forall (a_0, \bar{\mu}) \in \mathbb{P} \times \mathbb{S}^2$ and $\forall k \in \mathbb{N}$, there exists $\mathbb{P}_0 \subset \mathbb{P}$, a neighborhood of a_0 , $N(k) \in \mathbb{N}$ and a C^k -transformation*

$$\Psi_{(a,\bar{\mu})} : (r, \rho, \bar{y}) \longrightarrow (r, \rho, \psi_{(a,\bar{\mu})}(r, \rho, \bar{y}))$$

where

$$\psi_{(a,\bar{\mu})}(r, \rho, \bar{y}) = \bar{y} + o(|(r, \rho, \bar{y})|) \quad (2.26)$$

such that $\forall (a, \bar{\mu}) \in \mathbb{P}_0 \times \mathbb{S}^2$, the map $\psi_{(a,\bar{\mu})}$ transforms $X_{(a,\bar{\mu})}$ into one of the following normal forms:

- If $\sigma_1(a_0) \notin \mathbb{Q}$

$$\tilde{X}_{(a,\bar{\mu})} \begin{cases} \dot{r} &= -r \\ \dot{\rho} &= +\rho \\ \dot{y} &= -\bar{\sigma}_1(a, \bar{\mu}, \nu)y. \end{cases} \quad (2.27)$$

- If $\sigma_1(a_0) = \frac{p}{q} \in \mathbb{Q}$

$$\tilde{X}_{(a, \bar{\mu})} \begin{cases} \dot{r} &= -r \\ \dot{\rho} &= \rho \\ \dot{y} &= \frac{1}{q} \left[-p + \sum_{i=0}^{N(k)} \alpha_{i+1}(a, \bar{\mu}, \nu) (\rho^p y^q)^i \right] y \end{cases} \quad (2.28)$$

where $\nu = r\rho > 0$ and

$$\begin{aligned} \bar{\sigma}_1(a, \bar{\mu}, \nu) &= \sigma_1(a) - \alpha_0(a, \bar{\mu}, \nu) \\ \alpha_0(a, \bar{\mu}, \nu) &= \sum_{i=1}^{N(k)} \gamma_i \nu^i \\ \alpha_1(a, \bar{\mu}, \nu) &= p - \bar{\sigma}_1(a, \bar{\mu}, \nu)q \end{aligned} \quad (2.29)$$

where $\gamma_i(a, \bar{\mu})$, α_i and κ are smooth functions defined for $(a, \bar{\mu}) \in \mathbb{P}_0 \times \mathbb{S}^2$.

Proof. The proof [15] is a straightforward application of normal form theory. \square

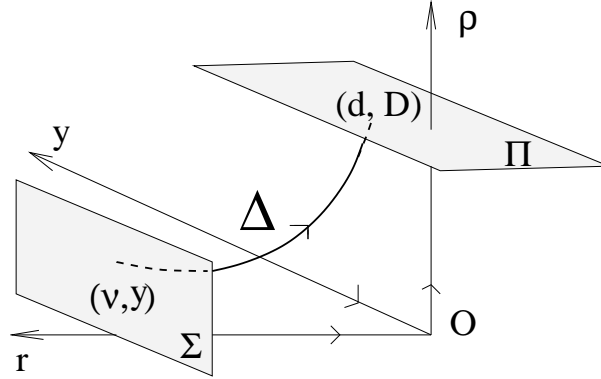


Figure 7: The first type Dulac map

We consider the first type Dulac map (Fig. 2.8):

$$\Delta_{(a, \bar{\mu})} = (d, D) : \Sigma \longrightarrow \Pi$$

where $\Sigma = \{r = r_0\}$ and $\Pi = \{\rho = \rho_0\}$ are sections in the normal form coordinates, r_0 and ρ_0 are positive constants.

To simplify the notation, for all the maps and vector fields, we will drop the index $(a, \bar{\mu})$. For example, the Dulac map $\Delta(\nu, \tilde{y}_1)$ means $\Delta_{(a, \bar{\mu})}(\nu, \tilde{y}_1)$.

If we parameterize the sections Σ and Π by (ν, y) with the obvious relation $\rho = \frac{\nu}{r_0}$ on Σ and $r = \frac{\nu}{\rho_0}$ on Π , then we have

Theorem 2.13. *For any $a_0 \in \mathbb{P}$ and $\bar{\mu} \in \mathbb{S}^2$, consider the family $\tilde{X} = \tilde{X}_{(a, \bar{\mu})}$ with eigenvalues $-1, 1, \sigma_1(a_0)$ in normal form (2.27) or (2.28). Then $\forall Y_0 \in \mathbb{R}$, there exist*

$\mathbb{P}_0 \subset \mathbb{P}$, a neighborhood of a_0 , and $\nu_1 > 0$ such that $\forall \nu \in (0, \nu_1)$ and $(a, \bar{\mu}, y) \in \mathbb{P}_0 \times \mathbb{S}^2 \times [0, Y_0]$, the Dulac map $\Delta(\nu, y) = (d(\nu, y), D(\nu, y))$ has the form

$$\begin{cases} d(\nu, y) &= \nu \\ D(\nu, y) &= \left(\frac{\nu}{\nu_0}\right)^{\bar{\sigma}_1} \left[y + \phi\left(\nu, \omega\left(\frac{\nu}{\nu_0}, -\alpha_1\right), y\right) \right] \end{cases} \quad (2.30)$$

where $\nu_0 = r_0 \rho_0 > 0$ a constant and

$$\begin{aligned} \text{If } \sigma_1(a_0) \notin \mathbb{Q}, \quad \phi &= 0; \\ \text{If } \sigma_1(a_0) = \frac{p}{q} \in \mathbb{Q}, \quad p, q \in \mathbb{N} \text{ and } (p, q) &= 1, \text{ then } \phi\left(\nu, \omega\left(\frac{\nu}{\nu_0}, -\alpha_1\right), y\right) \text{ is } C^\infty \text{ and} \\ \phi &= O\left(\nu^{\bar{p}} \omega^{q+1}\left(\frac{\nu}{\nu_0}, -\alpha_1\right) \ln \frac{\nu}{\nu_0}\right) \\ \frac{\partial \phi}{\partial y} &= O\left(\nu^{\bar{p}} \omega^q\left(\frac{\nu}{\nu_0}, -\alpha_1\right) \ln \frac{\nu}{\nu_0}\right) \\ \frac{\partial^j \phi}{\partial y^j} &= O\left(\nu^{\bar{p}(1 + [\frac{j-2}{q}])} \omega^{q-j+1+q[\frac{j-2}{q}]}\left(\frac{\nu}{\nu_0}, -\alpha_1\right) \ln \frac{\nu}{\nu_0}\right), \quad j \geq 2 \end{aligned} \quad (2.31)$$

where

$$\bar{p} = \begin{cases} q\bar{\sigma}_1(a, \nu) & \alpha_1 \geq 0 \\ p & \alpha_1 < 0. \end{cases} \quad (2.32)$$

Also all the partial derivatives with respect to the parameters $(a, \bar{\mu})$ are of order

$$O\left(\nu^{\bar{p}} \omega^q\left(\frac{\nu}{\nu_0}, -\alpha_1\right) \ln \frac{\nu}{\nu_0}\right).$$

Remark 2.14.

1. As the first component of Δ is the identity we only write the second component. We will do the same with the other transition maps.
2. Theorem 2.13 gives the inverse of the Dulac map $\Pi_2 \longrightarrow \Sigma_2$ near P_2 .
3. Essentially Theorem 2.13 ensures that the Dulac map behaves under derivation and composition with C^k maps as in the simple case where $a(0) \notin \mathbb{Q}$. Whenever there is no additional difficulty in the case $a(0) \in \mathbb{Q}$ compared to the case $a(0) \notin \mathbb{Q}$ and the ideas are very similar to [15] we will present the proof in the simple case $a(0) \notin \mathbb{Q}$, so as to enlighten the ideas.

Remark 2.15. In this paper, all the graphics through a nilpotent point are studied inside the global blown-up families with several parameters:

- case of a nilpotent point in the finite plane $a \in \mathbb{P}, \bar{\mu} = (\bar{\mu}_1, \bar{\mu}_2, \bar{\mu}_3) \in V \subset \mathbb{S}^2, \nu > 0$;
- case of a nilpotent point at infinity $A \in \mathbb{P}, \bar{\mu} = (\bar{\mu}_1, \bar{\mu}_2) \in V \subset \mathbb{S}^1, \nu > 0$.

We will simply denote all the parameters described above which relate to a graphic by λ . When we study the cyclicity of a graphic, we take a section Σ (sections Σ_1 and Σ_2) in the normal form coordinates in a neighborhood of a singular point, and we study the number of small zeros of the displacement map for the parameter λ in some subset (cone) of $\mathbb{P} \times \mathbb{S}^2 \times [0, \nu)$ for $\nu > 0$ sufficiently small.

Consider the transition map T_λ along the passage from P_1 to P_2 (in fact its second component). Let V_i be the subset of parameters in which the pp-graphics Eppi exists ($i = 1, 2, 3$). By Prop. 6.2 in [15], there exists $\nu_0 > 0$ such that for any $k \in \mathbb{N}$, if $\lambda \in V_3$ (resp. $\lambda \in V_2$) all the derivatives of T_λ (resp. T_λ^{-1}) are sufficiently small. For $\lambda \in V_1$, $T_\lambda(\tilde{y}_1)$ is C^k , and the transition has a “funnelling effect”, i.e. T_λ is almost affine.

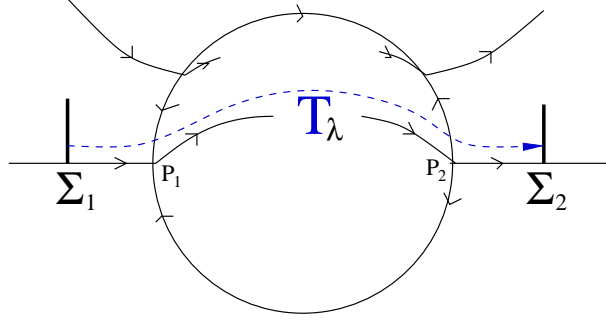


Figure 8: The transition map along the pp-passage: “funnelling effect”.

Theorem 2.16. [15] *There exists $\varepsilon_0 > 0$ such that for any $k \in \mathbb{N}$, $a_0 \in (0, \frac{1}{2})$, there exist $A_0 \subset (0, \frac{1}{2})$, a neighborhood of a_0 such that for $\forall (a, \bar{\mu}) \in A_0 \times V_3$, T'_λ is sufficiently small; while for $(a, \bar{\mu}) \in A \times V_2$, $(T_{\lambda^{-1}})'$ is sufficiently small. For any $(a, \bar{\mu}) \in A_0 \times V_1$ and $\nu > 0$ sufficiently small, T_λ is C^k , and*

$$T_\lambda(\tilde{y}_1) = \sum_{i=0}^k \gamma_{12i}(\lambda) \tilde{y}_1^i + O(y^{k+1}) \quad (2.33)$$

where

$$\begin{aligned} \gamma_{120} &= m_{120}(\nu) \left(\frac{\nu}{\nu_0} \right)^{-\bar{\sigma}_1} + \kappa_1 r_0^p (1 - m_{121}(\nu)) \omega \left(\frac{\nu}{\nu_0}, \alpha_1 \right) + O \left(\left(\frac{\nu}{\nu_0} \right)^{\bar{\sigma}_1} \omega^2 \left(\frac{\nu}{\nu_0}, -\alpha_0 \right) \right) \\ \gamma_{121} &= m_{121}(\nu) + O \left(\left(\frac{\nu}{\nu_0} \right)^{\bar{p}} \omega^q \left(\frac{\nu}{\nu_0}, -\alpha_0 \right) \ln \frac{\nu}{\nu_0} \right) \\ \gamma_{12i} &= O \left(\nu^{\bar{p}(1 + [\frac{i-2}{q}])} \omega^{q+1-i-q[\frac{i-2}{q}]} \left(\frac{\nu}{\nu_0}, -\alpha_0 \right) \ln \frac{\nu}{\nu_0} \right), \quad i \geq 2 \end{aligned}$$

where $m_{120}(0) = 0$ and $m_{121}(0) = \exp(\frac{\pi \bar{\mu}_3}{\sqrt{a \bar{\mu}_2}})$.

3 The finite cyclicity of the pp-graphics

In the proof of the finite cyclicity, we will always use $*$ to denote a positive constant.

3.1 Finite cyclicity of the codimension 3 graphic with an elliptic nilpotent point with pp-transition together with a hyperbolic saddle

Note that this graphic should figure in the zoo of Kotova-Stanzo in the generic case where the singular point has hyperbolicity ratio $\neq 1$ [11].

Theorem 3.1. *Consider a graphic with pp-transition through a nilpotent elliptic point of multiplicity 3 for which $a \neq \frac{1}{2}$ in (2.13) and a hyperbolic saddle. If the hyperbolic saddle has hyperbolicity ratio $\sigma \neq 1$, then the graphic has finite cyclicity at most 2.*

Proof. As shown in Tab. 2, to prove the graphic has finite cyclicity, we have to prove that all the limit periodic sets Epp1, Epp2 and Epp3 have finite cyclicity. We limit ourself to the case $\sigma > 1$.

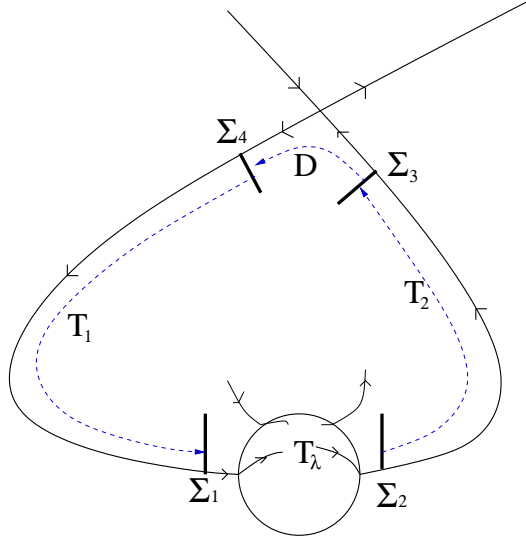


Figure 9: Graphic through a nilpotent elliptic point and a hyperbolic saddle

Let $T_\lambda : \Sigma_1 \longrightarrow \Sigma_2$ be the transition map in the neighborhood of the nilpotent point as defined in Theorem 2.16. Let V_i be the subset of parameters in which the pp-graphics Eppi exists ($i = 1, 2, 3$).

In the neighborhood of the hyperbolic saddle, take sections Σ_3 and Σ_4 using the normal form coordinates. By Prop. 2.5, the Dulac map $D : \Sigma_3 \longrightarrow \Sigma_4$ has the form

$$D(x, \lambda) = x^{\sigma(\lambda)}(1 + \phi(x, \lambda)) \quad (3.1)$$

where $\phi(x, \lambda) \in (I_0^\infty)$.

For the graphics Epp1 and Epp3, consider the displacement map defined from Σ_3 to Σ_2 :

$$\begin{aligned} L : \Sigma_3 &\longrightarrow \Sigma_2 \\ L &= T_\lambda \circ T_1 \circ D - T_2^{-1} \end{aligned} \quad (3.2)$$

where $T_1 : \Sigma_4 \longrightarrow \Sigma_1$ and $T_2 : \Sigma_2 \longrightarrow \Sigma_3$ are the regular transition maps using normal form coordinates on each section. By the chain rule,

$$L' = \sigma T_\lambda' T_1' x^{\sigma-1} (1 + \bar{\phi}(x, \lambda)) - (T_2^{-1})'.$$

The second term is bounded away from 0 while the first term is small which gives the finite cyclicity of the graphic is at most 1.

For the graphic Epp2, we consider the displacement map defined from Σ_3 to Σ_1 :

$$\begin{aligned} L : \Sigma_3 &\longrightarrow \Sigma_1 \\ L &= T_1 \circ D - T_\lambda^{-1} \circ T_2^{-1}. \end{aligned} \quad (3.3)$$

Then a straightforward calculation gives that

$$L(x, \lambda) = \tilde{m}_{10}(\lambda) + \tilde{m}_1(\lambda)x^{\sigma(\lambda)}[1 + \tilde{\phi}(x, \lambda)] - [\tilde{m}_{20}(\lambda) + \tilde{m}_2(\lambda)x(1 + O(x))] \quad (3.4)$$

where $\tilde{m}_1(\lambda_0)\tilde{m}_2(\lambda_0) \neq 0$, $\bar{\phi} \in (I_0^\infty)$ and $\tilde{m}_2(\lambda_0)$ is very small.

The first derivative of $L(x, \lambda)$ gives

$$L'(x, \lambda) = \sigma(\lambda)\tilde{m}_1(\lambda)x^{\sigma(\lambda)-1} \left(1 + \tilde{\phi}_1(x, \lambda)\right) - \tilde{m}_2(\lambda)[1 + O(x)] \quad (3.5)$$

where $\tilde{\phi}_1(x, \lambda) \in (I_0^\infty)$. Let $L_1(x, \lambda) = \frac{L'(x, \lambda)}{1+O(x)}$. Then by (3.5), $L'(x, \lambda) = 0$ is equivalent to $L_1(x, \lambda) = 0$. Since

$$L'_1(x, \lambda) = \tilde{m}_1(\lambda)\sigma(\lambda)(\sigma(\lambda) - 1)x^{\sigma(\lambda)-2} \left(1 + \tilde{\phi}_2(x, \lambda)\right) \neq 0$$

where $\tilde{\phi}_2(x, \lambda) \in (I_0^\infty)$, so $L(x, \lambda) = 0$ has at most 2 small positive roots which gives that the graphic has cyclicity at most 2. (A standard checking ensures that the case $\sigma(\lambda) = 2$ causes no problem.) \square

Corollary 3.2. *The graphics (I_{23}^2) , (I_{24}^2) and (I_{25}^2) have cyclicity ≤ 2 .*

Proof. This follows immediately from Theorem 3.1 since the graphics occur in family (2.17) with $A \neq \frac{1}{2}$ and the additional hyperbolic saddle at infinity has hyperbolicity ratio $\sigma = \frac{A}{1-A} \neq 1$ or $\frac{1}{\sigma}$. \square

3.2 Finite cyclicity of the hemicycles (H_6^1) and (H_9^3)

In order to prove the finite cyclicity of the hemicycles (H_6^1) and (H_9^3) , we will need to prove that some regular transition in these hemicycles has a nonzero second derivative. This is the purpose of the following lemma.

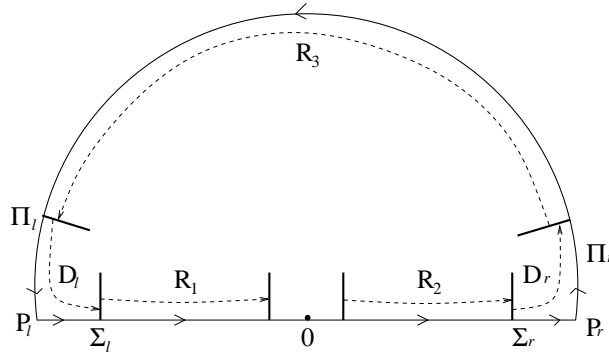


Figure 10: Transition maps related to the quadratic system (2.14)

Lemma 3.3. *Consider the quadratic system (2.14) with $a \in (0, \frac{1}{2})$, Fig. 10. The graphic (H_6^1) occurs for $c^2 - 4(1 - a) < 0$. We work under this hypothesis.*

1. Take sections $\Sigma_l = \{x = -X_0\}$, $\Sigma_1 = \{x = -x_0\}$, $\Sigma_2 = \{x = x_0\}$ and $\Sigma_r = \{x = X_0\}$, where $0 < x_0 < X_0$ constants. Let $R_1 : \Sigma_l \longrightarrow \Sigma_1 = \{x = -x_0\}$ and $R_2 : \Sigma_2 \longrightarrow \Sigma_r$ be the two regular transformations along the invariant line $y = 0$. Then

$$\begin{aligned} R_1(y) &= \left(\frac{x_0}{X_0}\right)^{1/a}, \\ R_2(y) &= \left(\frac{X_0}{x_0}\right)^{1/a}. \end{aligned} \quad (3.6)$$

2. Let $(v, w) = (\frac{x}{y}, \frac{1}{y})$. Then system (2.14) at infinity becomes

$$\begin{cases} \dot{v} &= (a-1)v^2 + cv - 1 + w \\ \dot{w} &= -vw. \end{cases} \quad (3.7)$$

Let $u_0 > 0$ small, $\Pi_l = \{v = -\frac{1}{u_0}\}$ and $\Pi_r = \{v = \frac{1}{u_0}\}$. Then the transformation map

$$R_3 : \Pi_r \longrightarrow \Pi_l$$

is C^∞ and if we write

$$R_3(w) = \beta_{001}(u_0)w + \beta_{002}(u_0)w^2 + O(w^3). \quad (3.8)$$

then

$$\begin{aligned} \beta_{001}(u_0) &= \exp(-c_2\pi) + O(u_0), \\ \beta_{002}(u_0) &= -\frac{\exp(-3c_2\pi)[\exp(c_2\pi) - 1]}{(2k_1 - 2)(1-a)^2} u_0^{2(k_2 - k_1 + 1)} [1 + O(u_0)] \end{aligned} \quad (3.9)$$

where

$$\begin{aligned} k_1 &= \frac{3-4a}{2(1-a)} \in (1, \frac{3}{2}) \\ k_2 &= \frac{1}{2(1-a)} \in (\frac{1}{2}, 1) \\ 2(k_2 - k_1 + 1) &= \frac{2a}{1-a} \in (0, 2) \\ c_1 &= \frac{\sqrt{4(1-a) - c^2}}{c} \\ c_2 &= \frac{1}{(1-a)\sqrt{4(1-a) - c^2}}. \end{aligned} \quad (3.10)$$

Proof. The proof for the first part is straightforward. We now prove the second part.

Note that for system (3.7), the w -axis is invariant, also with $0 < c < 2\sqrt{1-a}$, there holds $\dot{v}|_{w=0} = (a-1)v^2 + cv - 1 < 0$. Hence R_3 is a C^∞ map which can be written as (3.8). By Prop. 2.7, a straightforward calculation gives

$$\begin{aligned} \beta_{001} &= \exp\left(\int_{\frac{1}{u_0}}^{-\frac{1}{u_0}} \frac{v dv}{(1-a)v^2 - cv + 1}\right) \\ &= \exp\left(-c_2 \left[\arctan \frac{2(1-a)-cu_0}{c_1 u_0} - \arctan \frac{-2(1-a)-cu_0}{c_1 u_0} \right]\right) \left[\frac{(1-a)+cu_0+u_0^2}{(1-a)-cu_0+u_0^2} \right]^{k_2} \\ &= \exp(-c_2\pi) + O(u_0) \end{aligned} \quad (3.11)$$

and

$$\begin{aligned} \beta_{002}(u_0) &= -\beta_{001}(u_0) \int_{-\frac{1}{u_0}}^{\frac{1}{u_0}} \frac{2v \exp\left(\int_{\frac{1}{u_0}}^v \frac{v dv}{(1-a)v^2 - cv + 1}\right)}{((1-a)v^2 - cv + 1)^2} dv \\ &= -\frac{2u_0^{2k_2} [1+O(u_0)] \exp(-\frac{3c_2\pi}{2})}{(1-a)^{k_2}} \int_{-\frac{1}{u_0}}^{\frac{1}{u_0}} \frac{2v \exp\left(c_2 \arctan\left(\frac{2(1-a)v-c}{c_1}\right)\right)}{((1-a)v^2 - cv + 1)^{k_1}} dv \end{aligned} \quad (3.12)$$

where k_1, k_2, c_1 and c_2 are given by (3.10).

Note that

$$\lim_{u_0 \rightarrow 0} \frac{\int_{-\frac{1}{u_0}}^{\frac{1}{u_0}} \frac{2v \exp\left(c_2 \arctan\left(\frac{2(1-a)v-c}{c_1}\right)\right)}{((1-a)v^2 - cv + 1)^{k_1}} dv}{\frac{1}{u_0^{2k_1-2}}} = \frac{\exp(\frac{1}{2}c_2\pi) - \exp(-\frac{1}{2}c_2\pi)}{(2k_1-2)(1-a)^{k_1}}.$$

Therefore by (3.12), we have (3.9). \square

Theorem 3.4. *The hemicycle (H_6^1) has finite cyclicity.*

Proof. The hemicycle (H_6^1) occurs in (2.14) with $0 < c < 2\sqrt{1-a}$. After the blow-up of the family, take sections Σ_1 and Σ_2 in the normal form coordinates at the entrance and exit parabolic sectors in the neighborhood of P_1 and P_2 respectively (Fig. 11). To prove that (H_6^1) has finite cyclicity, we first study the transition map

$$R : \Sigma_2 \longrightarrow \Sigma_1 \quad (3.13)$$

along the equator. We are going to prove in detail that the second component $R_2(\lambda_0, \tilde{y}_2)$ is nonlinear in \tilde{y}_2 .

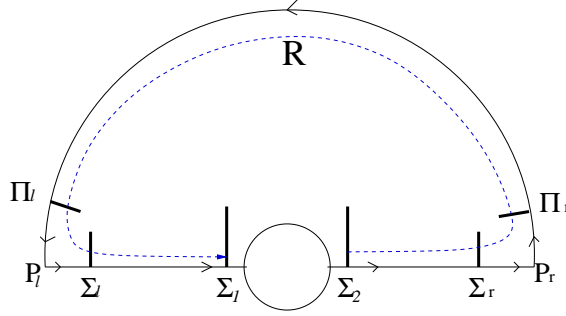


Figure 11: The hemicycle (H_6^1)

(1). Normal forms and Dulac maps at infinity

As shown in Fig. 11, let P_r be the saddle point at infinity in the direction of the positive x -axis. Using coordinates $(z_r, u_r) = (\frac{1}{x}, \frac{y}{x})$, we have

$$\begin{cases} \dot{u}_r &= u_r(1-a-cu_r+u_r^2-u_rz_r) \\ \dot{z}_r &= -z_r(a+cu_r-u_r^2+u_rz_r) \end{cases} \quad (3.14)$$

Hence P_r is a hyperbolic saddle of hyperbolicity ratio $\sigma_r = \frac{a}{1-a}$. For $a \in (0, \frac{1}{2})$, we have $0 < \sigma_r < 1$. Dividing system (3.14) by $1-a-cu_r+u_r^2-u_rz_r$ (positive in the neighborhood of P_r), a normalizing change of coordinates can be taken of the form $(u_r, z_r) = (u_r, \Psi_r(u_r, Z_r))$ where

$$\begin{aligned} \Psi_r(u_r, Z_r) &= d_{r1}(u_r)Z_r + d_{r2}(u_r)Z_r^2 + u_rO(Z_r^3) \\ &= [1+O(u_r)]Z_r + O(u_r)O(Z_r^2). \end{aligned} \quad (3.15)$$

Take two sections $\Sigma_r = \{Z_r = Z_0\}$ and $\Pi_r = \{u_r = u_0\}$ in the normal form coordinates. By [12], for the Dulac map $D_r : \Sigma_r \longrightarrow \Pi_r$, we have

$$D_r(u_r) = u_r^{\sigma_r}(A_r + \psi_r(u_r)) \quad (3.16)$$

where $A_r > 0$ constant, also $\psi_r \in (I_0^\infty)$.

To study P_l , the singular point at infinity in the direction of the negative x-axis, we use coordinates $(z_l, u_l) = (-\frac{1}{x}, -\frac{y}{x})$. The study is obtained from that of P_r by $(u_r, z_r) \mapsto (-u_l, -z_l)$, yielding a normalizing change of coordinates of the form

$$(u_l, Z_l) = (u_l, \Psi_l(u_l, z_l)) = d_{l1}(u_l)z_l + d_{l2}(u_l)z_l^2 + u_l O(z_l^3).$$

Taking two sections $\Pi_l = \{u_l = u_0\}$, $\Sigma_l = \{Z_l = Z_0\}$ in the normal form coordinates, the Dulac map $D_l : \Pi_l \longrightarrow \Sigma_l$ can be written as

$$D_l(Z_l) = Z_l^{\sigma_l}(A_l + \psi_l(Z_l)) \quad (3.17)$$

where $\sigma_l = \frac{1}{\sigma_r} > 1$, $A_l > 0$ constant, also $\psi_l \in (I_0^\infty)$.

(2). Decomposition of the map R

The transition map R defined in (3.13) can be calculated by the decomposition

$$R = R_1 \circ D_l \circ R_0 \circ D_r \circ R_2 \quad (3.18)$$

where R_1 and R_2 are the regular transition maps in the first part of Lemma 3.3 and R_0 is the map R_3 in the second part of Lemma 3.3 seen in different coordinates allowing the compositions. Then a straightforward calculation from (3.16), (3.17) and (3.18) gives

$$R(\tilde{y}) = \beta_1 \tilde{y} + \beta_2 \tilde{y}^{1+\sigma_r} + o(\tilde{y}^{1+\sigma_r}) \quad (3.19)$$

where

$$\begin{aligned} \beta_1 &= R'_1(0)R'_2(0)(A_r R'_0(0))^{\frac{1}{\sigma_r}} A_l > 0 \\ \beta_2 &= \frac{1}{2\sigma_r} R'_1(0)(R'_2(0))^{\sigma_r+1}(R'_0(0))^{\frac{1}{\sigma_r}-1} R''_0(0) A_l A_r^{1+\frac{1}{\sigma_r}}. \end{aligned} \quad (3.20)$$

(3). Calculation of $R''_0(0)$ to show $R(\tilde{y})$ is nonlinear

It follows from (3.19) and (3.20) that to show $R(\tilde{y})$ is nonlinear, it suffice to prove $R''_0(0) \neq 0$.

To do this, we introduce the coordinates $(v, w) = (\frac{x}{y}, \frac{1}{y})$ and make the following decomposition

$$R_0 := \bar{\Psi}_l \circ \Phi_2 \circ R_3 \circ \Phi_r \circ \bar{\Psi}_r \quad (3.21)$$

where we denote $\bar{\Psi}_r(Z_r) = \Psi_r(u_0, Z_r)$ and similarly $\bar{\Psi}_l(z_l) = \Psi_l(u_0, z_l)$, and

$$\Phi_r : \begin{cases} v = \frac{1}{u_r} \\ w = \frac{z_r}{u_r} \end{cases}, \quad \Phi_l : \begin{cases} u_l = -\frac{1}{v} \\ z_l = -\frac{w}{v} \end{cases} \quad (3.22)$$

are the coordinate changes between the charts.

It follows from (3.21), (3.22) and (3.8) that

$$R_0(Z_r) = \beta_{01} Z_r + \beta_{02} Z_r^2 + O(Z_r^3)$$

where

$$\begin{aligned}
\beta_{01}(u_0) &= d_{r1}(u_0)d_{l1}(u_0)\beta_{001} \\
&= e^{-c_2\pi} + O(u_0), \\
\beta_{02}(u_0) &= \beta_{001}d_{l1}(u_0)d_{r2}(u_0) + d_{l2}(u_0)d_{r1}^2(u_0)\beta_{001}^2 + \frac{1}{u_0}d_{r1}^2(u_0)d_{l1}(u_0)\beta_{002} \\
&= O(u_0) + O(u_0) - \frac{1}{u_0} \frac{\exp(-3c_2\pi)[\exp(c_2\pi) - 1]}{(2k_1 - 2)(1 - a)^2} u_0^{2(k_2 - k_1 + 1)} [1 + O(u_0)] \\
&= -\frac{\exp(-3c_2\pi)[\exp(c_2\pi) - 1]}{(2k_1 - 2)(1 - a)^2} u_0^{2(k_2 - k_1 + 1)} [1 + O(u_0)] + O(u_0).
\end{aligned}$$

Since

$$2(k_2 - k_1) + 1 = \frac{3a - 1}{1 - a} \in (-1, 1),$$

so $\beta_{02} \neq 0$. i.e., R has the form in (3.19) with $\beta_2 \neq 0$.

(4). Cyclicity of (H_6^1)

Note that all steps of the proof of Theorem 2.1 work with this form of the transition in (3.19), yielding $\text{Cycl}(H_6^1) \leq 2$. \square

Theorem 3.5. *The hemicycle (H_9^3) has finite cyclicity.*

Proof. For the hemicycle (H_9^3) , we have to prove that all the three limit periodic sets have finite cyclicity. The proof is similar to that of the (H_6^1) in the above theorem.

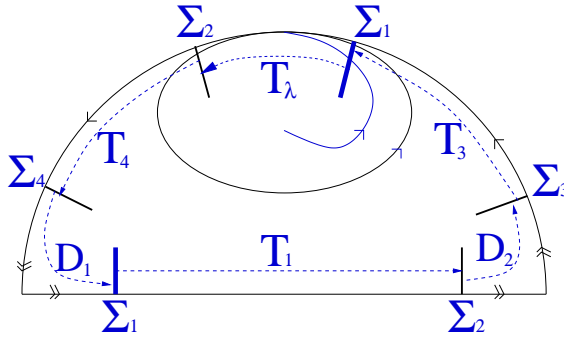


Figure 12: The hemicycle (H_9^3)

As shown in Fig. 12, take sections in the normal form coordinates in the neighborhood of the two hyperbolic saddles at infinity respectively.

We consider the transition map

$$\begin{aligned}
L : \bar{\Sigma}_1 &\longrightarrow \Sigma_1 \\
L &= D_1 \circ T_4 \circ T_\lambda - T_1^{-1} \circ D_2^{-1} \circ T_3^{-1}
\end{aligned}$$

where T_λ is the pp-transition through the nilpotent elliptic point, and as show in Fig. 12, the connections in T_λ , T_3 and T_4 are fixed while the connection T_1 can be broken. Note that $\sigma(0) = \frac{1-A}{A} < 1$ where $\sigma(0)$ is the hyperbolicity ratio of the left hyperbolic saddle point at infinity. A straightforward calculation gives that

$$\begin{aligned}
L(\tilde{y}, \lambda) &= \tilde{y}^{\sigma(\lambda)} [\bar{m}_1(\lambda) + \bar{m}_2(\lambda)\tilde{y} + O(\tilde{y}^2)] \\
&\quad - [m_0(\lambda) + m_1(\lambda)\tilde{y}^{\sigma(\lambda)} + m_2(\lambda)\tilde{y}^{2\sigma(\lambda)} + o(\tilde{y}^{2\sigma(\lambda)})]
\end{aligned} \tag{3.23}$$

where $m_2(\lambda) = * \frac{\partial^2 T_1^{-1}}{\partial y^2}$ and $m_1(\lambda)$ is bounded and bounded away from zero.

Differentiating of $L(\tilde{y}, \lambda)$ with respect to \tilde{y} yields

$$L'(\tilde{y}, \lambda) = \tilde{y}^{\sigma(\lambda)-1} [\sigma(\lambda)\bar{m}_1(\lambda) + (1 + \sigma(\lambda))\bar{m}_2(\lambda)\tilde{y} + O(\tilde{y}^2)] - \tilde{y}^{\sigma(\lambda)-1} [\sigma(\lambda)m_1(\lambda) + 2\sigma(\lambda)m_2(\lambda)\tilde{y}^{\sigma(\lambda)} + o(\tilde{y}^{\sigma(\lambda)})] \quad (3.24)$$

For Epp2, $\bar{m}_1(\lambda)$ is very large, hence $L'(\tilde{y}, \lambda) > 0$ for $\tilde{y} > 0$ small and λ small. For Epp3, $\bar{m}_1(\lambda)$ is very small, hence $L'(\tilde{y}, \lambda) < 0$ for $\tilde{y} > 0$ small and λ small. Therefore Epp2 and Epp3 have cyclicity at most 1.

We now consider the case of Epp1. Let

$$L_1(\tilde{y}, \lambda) = \tilde{y}^{1-\sigma(\lambda)} L'(\tilde{y}, \lambda).$$

Then the number of small roots of $L(\tilde{y}, \lambda) = 0$ is at most 1 plus the number of roots of $L_1(\tilde{y}, \lambda) = 0$. Since $0 < \sigma(\lambda) < 1$, so

$$L'_1(\tilde{y}, \lambda) = -2\sigma(\lambda)m_2(\lambda)\tilde{y}^{\sigma(\lambda)-1} \left(1 + o(\tilde{y}^{\sigma(\lambda)})\right) + (1 + \sigma(\lambda))\bar{m}_2(\lambda) + O(\tilde{y}) \neq 0$$

which gives that the number of small positive roots of $L(\tilde{y}, \lambda) = 0$ is at most 2, i.e. $Cycl(H_9^3) \leq 2$, if we show that $m_2(\lambda_0) \neq 0$.

Let us now show that $m_2(0) \neq 0$. The graphic occurs inside the family (2.17) with $\gamma = 0$. By Theorem 2.11, the invariant line $y = -1$ is part of the hemicycle. The transition map $T_1 : \Sigma_2 \rightarrow \Sigma_1$ along the invariant line then can be decomposed as

$$T_1 = \Phi_1 \circ T_0 \circ \Phi_2^{-1}(U, \lambda) \quad (3.25)$$

where Φ_1 and Φ_2 are the normalizing coordinates changes on the sections Σ_1 and Σ_2 respectively and U is the normalizing coordinate (see below). Let the sections Σ_i ($i = 1, 2$) be given by $z = z_0$ with $z_0 > 0$ small, then

$$T_0 : \{x = -\frac{1}{z_0}\} \rightarrow \{x = \frac{1}{z_0}\}$$

is the regular transition map along the invariant line $y = -1$ for the system (2.17) with $\delta^2 - 4A < 0$.

Note that for system (2.17), if we move the invariant line $\hat{y} = -1$ to $y = 0$ by making the transformation

$$x = -\hat{x}, \quad y = \hat{y} - 1,$$

then system (2.17) becomes

$$\begin{cases} \dot{\hat{x}} &= -\delta\hat{x} + \hat{y} - 1 - A\hat{x}^2 \\ \dot{\hat{y}} &= -\hat{x}\hat{y}. \end{cases} \quad (3.26)$$

System (3.26) is exactly the system (3.7) if we take $A = 1 - a$ and $\delta = -c$. Hence the calculation of the transition map along the invariant line $\hat{y} = 0$ can be done as before. We need also consider the normalizing changes of coordinates. For that purpose we transform (3.26) by means of $(u, z) = (\frac{y}{x}, \frac{1}{x})$. This yields the system

$$\begin{cases} \dot{u} &= (A - 1)u + \delta uz - u^2 z - uz^2 \\ \dot{z} &= Az + \delta z^2 + z^3 - uz^2. \end{cases} \quad (3.27)$$

In order to bring to normalizing coordinates we divide the system by $A + \delta z + z^2 - uz^2$. Hence normalizing coordinates can be taken as

$$(U, Z) = \left(1 + O(z)u + O(z)O(u^2), z \right).$$

As in part (3) in Theorem 3.4, we can conclude that $m = m_2(\lambda_0) \neq 0$. \square

3.3 Finite cyclicity of a graphic with a nilpotent elliptic point, a saddle and a saddle-node

Theorem 3.6. *A graphic with a pp-transition through a nilpotent elliptic point together with an attracting saddle node and a repelling hyperbolic saddle (with hyperbolicity ratio $\sigma < 1$) has finite cyclicity ≤ 2 provided that the saddle is located on the side of the parabolic sector of the saddle-node (Fig. 13).*

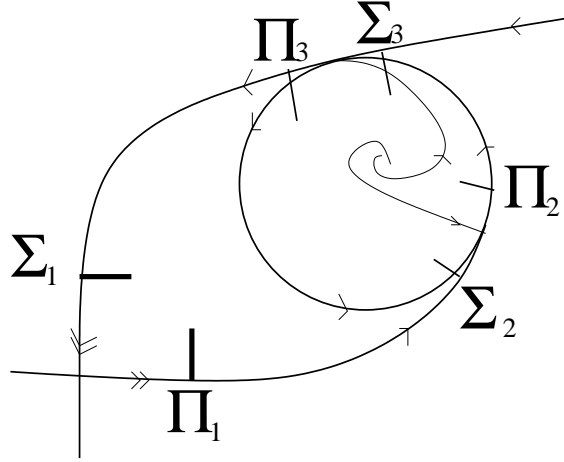


Figure 13: Graphic with a pp-transition, hyperbolic saddle and a saddle node

Proof. We take two sections Σ_1 and Π_1 located at the entrance and the exit of the saddle and other sections as in Fig. 13. Let

$$\begin{aligned} R_1 : \Pi_1 &\longrightarrow \Sigma_2 \\ R_2 : \Pi_2 &\longrightarrow \Sigma_3 \\ R_5 : \Pi_3 &\longrightarrow \Sigma_1 \end{aligned}$$

be the regular transition maps. The map from $\Sigma_3 \longrightarrow \Pi_3$ has the form (for a irrational)

$$\nu^{-\sigma_1} R_{4,\lambda}(M(\lambda) R_{3,\lambda}(\nu^{\sigma_1} \hat{g}))$$

where $M(\lambda)$ is 1 (resp. large, small) for Epp1 (resp. Epp2, Epp3) and $R_{3,\lambda}$, $R_{4,\lambda}$ are regular transitions, hence diffeomorphisms such that $R'_{3,\lambda}$ and $R'_{4,\lambda}$ are bounded and bounded away from 0.

We consider the displacement map

$$V_\lambda : \Pi_1 \longrightarrow \Sigma_1.$$

Here again we write the proof for a irrational which implies $\sigma(0)$ irrational but we explain what is the non trivial adaptation for the case $\sigma(0) = \frac{1}{2}$. The displacement map has the form

$$V_\lambda(y) = R_{5,\lambda} \left(\nu^{-\sigma_1} R_{4,\lambda} \left(M(\lambda) R_{3,\lambda} (\nu^{\sigma_1} R_{2,\lambda} (m(\lambda) R_{1,\lambda}(y))) \right) \right) - y^{\frac{1}{\sigma(\lambda)}} \quad (3.28)$$

where the $R_{i,\lambda}$ are regular transitions satisfying $R'_{i,\lambda}(y) \neq 0$ and $m(\lambda) \rightarrow 0$ as $\lambda \rightarrow 0$. Then

$$V'_\lambda(y) = m(\lambda) M(\lambda) R'_{1,\lambda} R'_{2,\lambda} R'_{3,\lambda} R'_{4,\lambda} R'_{5,\lambda} - \frac{1}{\sigma(\lambda)} y^{\frac{1}{\sigma(\lambda)} - 1}. \quad (3.29)$$

We divide a neighborhood of 0 in parameter space in two cones. In the first cone where $M(\lambda)m(\lambda) > \frac{1}{2}$, then $V'_\lambda(y) > 0$ for small y yielding cyclicity ≤ 1 . Note that this cone contains the values of parameter λ corresponding to Epp1 and Epp3.

In the second cone where $M(\lambda)m(\lambda) < 1$ then zeros of $V'_\lambda(y)$ are zeros of

$$W_\lambda(y) = \sigma(\lambda) M(\lambda) m(\lambda) - \frac{y^{\frac{1}{\sigma(\lambda)} - 1}}{R'_{1,\lambda} R'_{2,\lambda} R'_{3,\lambda} R'_{4,\lambda} R'_{5,\lambda}}. \quad (3.30)$$

Then for $\sigma(0) \neq \frac{1}{2}$

$$W'_\lambda(x) = - \left[\frac{1}{\sigma(\lambda)} - 1 \right] x^{\frac{1}{\sigma(\lambda)} - 2} \left[\hat{M}(\lambda) + O(M(\lambda)m(\lambda))O(x) + O(m(\lambda))O(x) \right] \quad (3.31)$$

where $\hat{M}(\lambda) \neq 0$. Then $W'_\lambda(x)$ is nonzero for small nonzero y .

In the particular case $\sigma(0) = \frac{1}{2}$, we apply the same argument but we replace the function $W_\lambda(y)$ by the function

$$\bar{W}_\lambda(y) = [\sigma(\lambda) M(\lambda) m(\lambda)]^{\frac{1}{2}} - \left[\frac{x^{\frac{1}{\sigma(\lambda)} - 1}}{R'_{1,\lambda} R'_{2,\lambda} R'_{3,\lambda} R'_{4,\lambda} R'_{5,\lambda}} \right]^{\frac{1}{2}}. \quad (3.32)$$

□

Corollary 3.7. *The graphic (I_{39}^2) has finite cyclicity.*

Proof. The graphic (I_{39}^2) occurs inside the family (2.17) with $\frac{1}{2} < A < 1$ and the hyperbolicity ratio is $\frac{1-A}{A} < 1$. The finite cyclicity of (I_{39}^2) follows from Theorem 3.6. □

3.4 Finite cyclicity of a graphic with a nilpotent elliptic point and a saddle-node

Theorem 3.8. *A graphic with a nilpotent elliptic point of multiplicity 3, a pp-transition, and a saddle-node with central transition has finite cyclicity if the regular transition from the nilpotent point to the node sector of the saddle-node is nonlinear.*

Proof. The graphics Epp1 and Epp3 have cyclicity 1 as the first return map P satisfies $P'(0) < 1$. We now consider the case of Epp2. As shown in Fig. 14, we take sections Σ_i

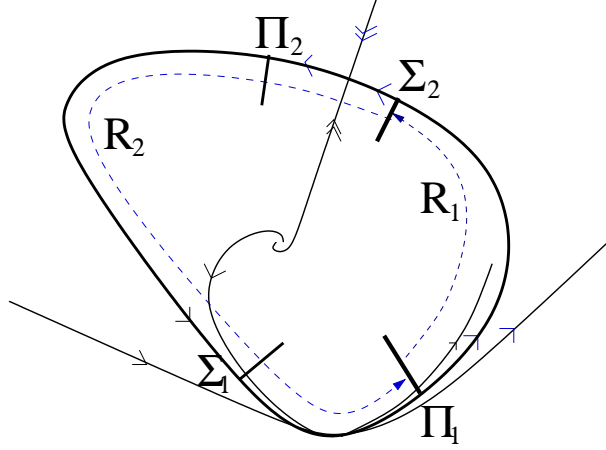


Figure 14: Graphic through a nilpotent elliptic point and a saddle-node

and Π_i ($i = 1, 2$) in normal form coordinates in the neighborhood of the elliptic point and the saddle-node respectively. Let

$$\begin{aligned} R_1 : \Pi_1 &\longrightarrow \Sigma_2 \\ R_2 : \Pi_2 &\longrightarrow \Sigma_1 \end{aligned}$$

be the regular transition maps. By assumption there exists N such that the transition map R_1 can be written as

$$R_1(y, \lambda) = \sum_{i=0}^N m_i(\nu, \lambda) y^i + O(y^{N+1}) \quad (3.33)$$

where $m_N(0, \lambda) \neq 0$.

We will consider the displacement map $V : \Pi_1 \longrightarrow \Sigma_2$. As in the proof of Theorem 3.6, the transition map through the blown-up sphere has the form

$$R_0(\hat{y}, \lambda) = \nu^{-\sigma_1} R_{4,\lambda}(M(\lambda) R_{3,\lambda}(\nu^{\sigma_1} \hat{y})). \quad (3.34)$$

where $M(\lambda)$ is large. It follows from Proposition 2.6 that the central transition map through the saddle-node has the form (2.8) with the constant $m(\lambda)$ small.

The displacement map V now reads

$$\begin{aligned} V(y, \lambda) &= R_1(y, \lambda) - m^{-1}(\lambda) R_2^{-1} \circ R_0^{-1}(y, \lambda) \\ &= R_1(y, \lambda) - m^{-1}(\lambda) R_2^{-1} \left(\nu^{-\sigma_1} R_{3,\lambda}^{-1} (M(\lambda)^{-1} R_{4,\lambda}^{-1} (\nu^{\sigma_1} y)) \right). \end{aligned} \quad (3.35)$$

Then

$$\begin{aligned} V'(y, \lambda) &= R_1'(y, \lambda) - m^{-1}(\lambda) R_2^{-1'} \left(R_0^{-1}(y, \lambda) \right) R_0^{-1'}(y, \lambda) \\ &= R_1'(y, \lambda) - m^{-1}(\lambda) M(\lambda)^{-1} R_2^{-1'} \left(R_0^{-1}(y, \lambda) \right) (R_{4,\lambda}^{-1})' (R_{3,\lambda}^{-1})'. \end{aligned} \quad (3.36)$$

Let

$$W(y, \lambda) = \frac{R_1'(y, \lambda)}{R_2^{-1'} \left(R_0^{-1}(y, \lambda) \right) (R_{4,\lambda}^{-1})' (R_{3,\lambda}^{-1})'} - m^{-1}(\lambda) M^{-1}(\lambda). \quad (3.37)$$

It follows from Theorem 2.16, (3.33) and (3.34) that $W^{(N-1)}(y, \lambda) \neq 0$ as all the higher order derivatives of R_0 and R_2 are small for small y because of the funnelling effect. This gives that the cyclicity of the graphic is at most N . \square

Since we will have to deal with family of graphics of the same type, we state the following important principle which will be used to deal with all the families of graphics.

Theorem 3.9. Analytic extension principle to prove a regular transition map is nonlinear:

The transition map must be calculated in normalizing coordinates on sections parallel to the axes.

1. *For the points P_i we deal with 3-dimensional hyperbolic saddles with two eigenvalues of the same sign and for which the planes $r = 0$ and $\rho = 0$ are invariant. Using Poincaré theorem stating that it is possible to bring a node to normal form via an analytic change of coordinates it is possible to choose normalizing coordinates which are analytic in the coordinate plane where the singular point has a node behavior. Our section is then analytic and parameterized by an analytic coordinate inside that plane (details in [15]).*
2. *Using the sectorial normalizing theorem for a saddle-node it is possible to show that there exist a normalizing change of coordinates which is analytic in the node sector for the zero value of the parameters. Then the section parallel to the stable (unstable) manifold in the node sector is analytic for the zero value of the parameters and parameterized by an analytic coordinate (details in [3]).*

Then the principle says: if a regular transition appears for a graphic in a family of graphics and if the two sections on which it is defined are analytic and parameterized by analytic coordinates, then, if the transition is nonlinear in one point, it is nonlinear everywhere.

It is usually easy to prove the nonlinearity of the transition near one of the boundary graphics of the family.

By the above Analytic extension principle and the finite cyclicity results obtained above, we immediately have

Corollary 3.10. *The graphics (F_{6a}^1) , (I_{5a}^1) , (I_{7a}^1) , (I_{8a}^1) , (I_{9a}^1) and (I_{10a}^1) have finite cyclicity.*

Proof. Since the pp-transition through the nilpotent elliptic point is almost affine, to prove the finite cyclicity of these graphics we only need to verify that the corresponding “external” map is nonlinear.

1. (F_{6a}^1) and (I_{5a}^1)

In the proof of Theorem 3.4 we show that the map R along the hemicycle (H_6^1) is nonlinear of order 2, therefore by Theorem 3.9, the corresponding transition for each of the graphic in the family (F_{6a}^1) is nonlinear too.

The nonlinearity of the corresponding map for (I_{5a}^1) comes from the proof of Theorem 3.5 for the hemicycle (H_9^3) and the fact that the regular transition map along the invariant line is nonlinear of order 2.

2. (I_{7a}^1) , (I_{8a}^1) , (I_{9a}^1) and (I_{10a}^1)

These graphics occur in family (2.17) with $A \neq \frac{1}{2}$ and the additional hyperbolic saddle at infinity has hyperbolicity ratio $\sigma = \frac{A}{1-A} \neq 1$. Thus the corresponding maps for the boundary graphics (I_{23}^2) , (I_{24}^2) , (I_{25}^2) and (I_{39}^2) are nonlinear respectively.

□

Remark 3.11. In [3], Dumortier, Ilyashenko and Rousseau proved that the graphic (I_{10a}^1) has finite cyclicity.

3.5 Finite cyclicity of the hemicycles (H_7^3) and (H_{10}^3)

Consider the hemicycle (H_7^3) . As shown in Fig. 15, take the transversal sections Π_2 and Π_0 in the neighborhood of the saddle point at infinity and the attracting saddle-node on the equator. Let

$$R_{3,0} : \Pi_2 \longrightarrow \Pi_0$$

be the regular transition map in the normalizing coordinates.

Theorem 3.12. *If $R_{3,0}''(0) \neq 0$, then the hemicycle (H_7^3) has finite cyclicity ≤ 2 .*

Proof. We write the proof in the case $a \in \mathbb{P}$ irrational. Then the hyperbolicity ratios of the two saddle points at infinity on the right (resp. left) are $\sigma_r = \frac{a}{1-a}$ (resp $\sigma_l = \frac{1}{\sigma_r}$) with $\sigma_r(0) < 1$ irrational.

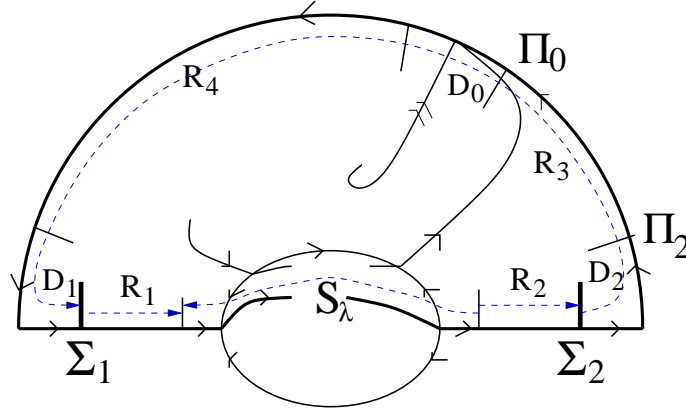


Figure 15: The transition maps of hemicycle (H_7^3) in proving its finite cyclicity

As shown in Fig. 15, let $R_{1,\lambda}$ (resp. $R_{2,\lambda}$) be the regular transitions along the x -axis on the left (resp. right). We can suppose that the transition $R_{4,\lambda}$ along the equator to the left of the saddle-node is the identity (see [9]). Let $R_{3,\lambda}$ be the transition along the equator on the right side of the saddle-node. In particular $R_{3,\lambda}(0) = 0$. The Dulac maps D_1 and D_2 have the form of (2.3) in Proposition 2.5 with $\psi_i = 0$. If we denote the central transition map of the saddle-node by D_0 and write it as in (2.8) with the coefficient $m_1(\lambda) \rightarrow 0$, then, the transition $\Sigma_2 \longrightarrow \Sigma_1$ along the equator can be written as

$$\begin{aligned} R_\lambda(y) &= D_1 \circ R_{4,\lambda} \circ D_0 \circ R_{3,\lambda} \circ D_2 \\ &= [m_1(\lambda) R_{3,\lambda}((R_{2,\lambda}(y))^{\sigma_r})]^{\sigma_l}. \end{aligned}$$

Let S_λ be the inverse of the transition map T_λ defined in (2.33). Consider the displacement map $V_\lambda : \Sigma_2 \rightarrow \Sigma_1$ given by

$$V_\lambda(y) = R_\lambda(y) - R_1^{-1} \circ S_\lambda \circ R_{2,\lambda}^{-1}(y).$$

The first derivative of R_λ is small for small y and the first derivative of S_λ is nonzero (resp. small, large) for Epp1 (resp. Epp2, Epp3). Hence for limit periodic sets of type Epp1 or Epp3, the displacement map has a nonzero derivative, yielding cyclicity ≤ 1 .

For Epp2, it follows from (2.33) that we can rewrite the map $S_\lambda(y_1)$ (we will apply this with $y_1 = R_{2,\lambda}^{-1}(y)$) as

$$S_\lambda(y_1) = \nu^{-\sigma_1} \left(\varepsilon_0 + m_2(\lambda) \nu^{\sigma_1} y_1 \left(1 + O(|(\nu^{\sigma_1}, m_2(\lambda))|) O(y_1) \right) \right),$$

with $m_2(\lambda) \rightarrow 0$ as $\lambda \rightarrow 0$. Hence

$$S'_\lambda(y_1) = m_2(\lambda) (1 + O(|(\nu^{\sigma_1}, m_2(\lambda))|) O(y_1)) = m_2(\lambda) (1 + \psi(y_1, \lambda))$$

where $\psi(y_1, \lambda) = O(\nu^{\sigma_1} m_2(\lambda))$. Moreover for $y_1 = R_{2,\lambda}^{-1}(y)$ we will have

$$1 + \psi(y_1, \lambda) = 1 + \psi_1(y, \lambda),$$

where again $\psi_1(y, \lambda) = O(\nu^{\sigma_1} m_2(\lambda))$.

Let

$$\begin{aligned} W_\lambda(y) &= \frac{V'_\lambda(y)}{m_1(\lambda) (1 + \psi_1(y, \lambda)) (R_{1,\lambda}^{-1})' (R_{2,\lambda}^{-1})'} \\ &= \frac{R'_\lambda(y)}{m_1(\lambda) (1 + \psi_1(y, \lambda)) (R_{1,\lambda}^{-1})' (R_{2,\lambda}^{-1})'} - \frac{m_2(\lambda)}{m_1(\lambda)} \\ &= a_0(\lambda) + a_1(\lambda) y^{\sigma_r(\lambda)} + O(y) \end{aligned} \tag{3.38}$$

where $a_1(\lambda) = *R''_{3,\lambda}(0)$ is bounded and bounded away from 0 for small z and λ as $R''_{3,0}$ is nonzero (see Lemmas 3.14 and 3.15 below). Hence $W'_\lambda(y)$ is large for small y and λ , yielding that (H_7^3) has cyclicity at most 2. \square

We will postpone the proof that $R_{3,0}$ after the proof of the finite cyclicity of (H_{10}^3) . The difference between (H_7^3) and (H_{10}^3) is that the transition map along the invariant line is not fixed in (H_{10}^3) while the transition along the equator was fixed in (H_7^3) . As shown in Fig. 16, let

$$R_{1,0} : \Sigma_1 \rightarrow \hat{\Sigma}_1$$

be the regular transition map from the saddle point to the attracting saddle-node in the normalizing coordinates. Similar to the case of (H_7^3) , we will show that it is sufficient to prove that $R''_{1,0}(0) \neq 0$. This will be proved in Lemma 3.15.

Theorem 3.13. *The hemicycle (H_{10}^3) has finite cyclicity ≤ 2 if $R''_{1,0}(0) \neq 0$.*

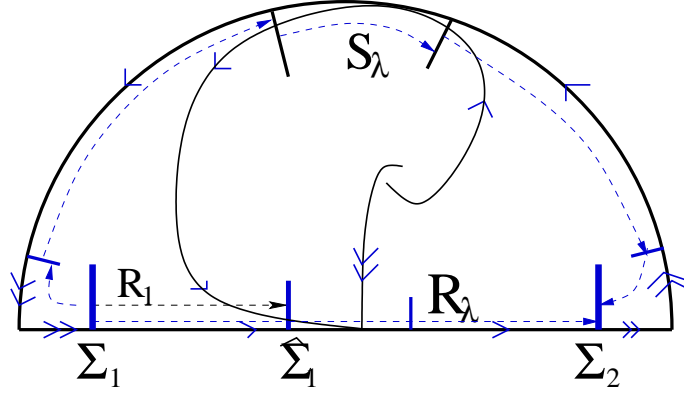


Figure 16: The transition maps for the hemicycle (H^3_{10})

Proof. Again, we write the proof in the case $A \in \mathbb{P}$ irrational. As shown in Fig. 16, we take two sections Σ_1 and Σ_2 near the hyperbolic saddles at infinity using the normalizing coordinates. Then we consider the displacement map

$$V_\lambda(y) = R_\lambda(y) - G_\lambda(y) : \Sigma_1 \longrightarrow \Sigma_2 \quad (3.39)$$

where R_λ is the transition from Σ_1 to Σ_2 along the invariant line, G_λ is the transition map along the equator (which is the composition of two regular transitions along the equator and the transition map S_λ through the nilpotent elliptic point) composed with the two Dulac maps near the hyperbolic saddles at infinity.

A straightforward calculation gives

$$R_\lambda(y) = \epsilon_0 + m_1(\lambda)[y + M_2 y^2 + O(y^3)] \quad (3.40)$$

where $m_1(\lambda) \rightarrow 0$ and $M_2(0) = *R''_{1\lambda}(0)$.

For the transition map G , note that the transition map T_λ through the nilpotent elliptic point is almost linear since it also satisfies $T_\lambda(0) = 0$. So, we can write the inverse of the transition map T as

$$S_\lambda(y_1) = m_2(\lambda)y_1(1 + O(|(\nu^\sigma, m_2(\lambda))|)O(y_1)) = m_2(\lambda)y_1(1 + \psi(y_1, \lambda)),$$

with $m_2(\lambda)$ nonzero (resp. small, large) for Epp1 (resp. Epp2, Epp3). Therefore, we can write the transition map G_λ as

$$G_\lambda(y) = \hat{m}_2(\lambda)y(1 + \hat{M}_2 y^{\sigma_r} + O(y^{1+\sigma_r})) \quad (3.41)$$

where $\sigma_r = \frac{A}{1-A} > 1$ and $\hat{m}_2(\lambda) = *m_2(\lambda)$.

Using the expression of (3.40) and (3.41) in (3.39), we have

$$V'_\lambda(y) = m_1(\lambda)[1 + 2M_2 y + O(y^2)] - \hat{m}_2(\lambda)[1 + \sigma_r \hat{M}_2 y^{\sigma_r} + O(y^{1+\sigma_r})]. \quad (3.42)$$

Hence for the limit periodic sets of type Epp1 and Epp3, $V'_\lambda(y) \neq 0$ for y and λ small, yielding cyclicity ≤ 1 .

For the limit periodic set of type Epp2, $\hat{m}_2(\lambda) = *m_2(\lambda)$ is small. Let

$$W_\lambda(y) = \frac{V'_\lambda(y)}{\hat{m}_2(\lambda)[1 + 2M_2y + O(y^2)]} = \frac{m_1(\lambda)}{\hat{m}_2(\lambda)} - \frac{1 + \sigma_r \hat{M}_2 y^{\sigma_r} + O(y^{1+\sigma_r})}{1 + 2M_2y + O(y^2)}.$$

Then

$$W_\lambda(y) = \frac{m_1(\lambda)}{\hat{m}_2(\lambda)} - 1 + 2M_2y + O(y^2) + O(y^{\sigma_r}) \quad (3.43)$$

where $M_2 = *R''_{1\lambda}(0)$. Therefore for y and λ sufficiently small

$$W'_\lambda(y) = 2M_2 + O(y) + O(y^{\sigma_r-1}).$$

Hence (H_{10}^3) has cyclicity at most 2 if $M_2 = R''_{1\lambda}(0) \neq 0$. \square

Next we show the nonlinearity of the two transition maps in the above two theorems.

It follows from the results in Section 2.6 that the hemicycle (H_{10}^3) occurs in the family

$$\begin{cases} \dot{x} &= -y + Ax^2 + 2\sqrt{A}x + 1, \\ \dot{y} &= xy \end{cases} \quad (3.44)$$

with $\frac{1}{2} < A < 1$, while (H_7^3) occurs in the family

$$\begin{cases} \dot{x} &= y + ax^2 + 2\sqrt{1-a}xy - y^2, \\ \dot{y} &= xy, \end{cases} \quad (3.45)$$

with $a \in (0, \frac{1}{2})$. If we calculate the regular transition map $R_{3\lambda}$ for (H_7^3) using system (3.45) by relocating system through $x = \frac{v}{w}$, $y = \frac{1}{w}$, we have system

$$\begin{cases} \dot{v} &= w + (a-1)v^2 + \sqrt{1-av} - 1, \\ \dot{w} &= vw. \end{cases} \quad (3.46)$$

A further change $v \mapsto -v$ can bring (3.46) to exactly system (3.44). Hence the calculation of $R_{3,0}$ is the same as the calculating for $R_{1,0}$ using system (3.44), yielding

Lemma 3.14. *The condition $R''_{3,0}(0) \neq 0$ is satisfied for (H_7^3) if and only if $R''_{1,0}(0) \neq 0$ for (H_{10}^3) .*

Note that system (3.44) has a saddle-node at $(-\frac{1}{\sqrt{A}}, 0)$. To make the calculations easier, we first translate the saddle-node to the origin. Then a rescaling

$$x \mapsto -A\sqrt{A}x, \quad y \mapsto -A^2y, \quad t \mapsto -\frac{1}{\sqrt{A}}t$$

yields

$$\begin{cases} \dot{x} &= y + x^2, \\ \dot{y} &= y(1 + Bx) \end{cases} \quad (3.47)$$

where $B = \frac{1}{A} \in (1, 2)$.

For system (3.47), we have a hemicycle (Fig. 17). As shown in the figure, let Σ_1 and Σ_2 be two sections parameterized by the normalized coordinates in the neighborhood of the repelling saddle-node and hyperbolic saddle at infinity respectively. One can see

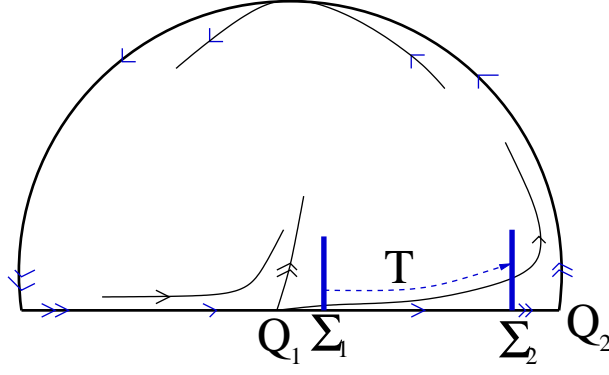


Figure 17: The transition map T for system (3.47) in Lemma 3.15

that to show $R''_{1,0}(0) \neq 0$ for (H^3_{10}) using system (3.44), it is equivalent to show that the transition map

$$T : \Sigma_1 \longrightarrow \Sigma_2$$

in the normalizing coordinates satisfies $T''(0) \neq 0$.

Lemma 3.15. *The transition map T has a nonzero second derivative, i.e., $T''(0) \neq 0$.*

Proof. Let us call (X, Y) (resp. (U, Z)) the normalizing coordinates at Q_1 , the origin (resp. Q_2 , the point at infinity). The regular transition map R can be written as a composition of the following 6 maps:

- 1) The map T_1 from $\{X = X_1\}$ to $\{x = x_0\}$ in the (X, Y) coordinates, where $(X_1, 0)$ and $(x_0, 0)$ represent the same point with (X, Y) and (x, y) coordinates respectively. Both sections are parameterized by Y . Hence $T'_1(0) = 1$.
- 2) The map T_2 which is the change of coordinates from Y to y on $\{x = x_0\}$. Then

$$T_2(Y) = a_1 Y + a_2 Y^2 + O(Y^3) \quad (3.48)$$

where $a_1 > 0$.

- 3) The map $T_3(y)$ which is the transition from $\{x = x_0\}$ (x_0 small) to $\{x = X_0\}$ (X_0 large) in (x, y) coordinates.

- 4) The map T_4 which is the transition from the coordinate y to the coordinate $u = \frac{y}{X_0}$ on $\{x = X_0\}$. Then T_4 is linear: $T_4(y) = \frac{y}{X_0} = Z_0 y$ with $Z_0 = \frac{1}{X_0}$ (the section $\{x = X_0\}$ becomes $\{z = Z_0\}$ in the $(u, z) = (\frac{y}{x}, \frac{1}{x})$ coordinates.

- 5) The change of coordinate T_5 from u to U on $\{z = Z_0\}$. Then

$$T_5(u) = b_1 u + b_2 u^2 + O(u^3) \quad (3.49)$$

where $b_1 > 0$.

- 6) The map T_6 from the image of $\{z = Z_0\}$ in (U, Z) coordinates to $\{Z = Z_1\}$ where $(0, Z_0)$ and $(0, Z_1)$ represent the same point written respectively in (u, z) and (U, Z) coordinates. Then $T'_6(0) = 1$.

Hence

$$T = T_6 \circ T_5 \circ T_4 \circ T_3 \circ T_2 \circ T_1. \quad (3.50)$$

A straightforward calculation from (3.48), (3.49) and (3.50) gives

$$T'(0) = \prod_{i=1}^6 T'_i(0) = \frac{a_1 b_1}{X_0} T'_3(0) \quad (3.51)$$

and

$$T''(0) = T'(0) \left[T''_1(0) + \frac{2a_2}{a_1} + \frac{T''_3(0)}{T'_3(0)} a_1 + \frac{2a_1 b_2}{b_1} Z_0 T'_3(0) + a_1 b_1 Z_0 T'_3(0) T''_6(0) \right]. \quad (3.52)$$

Now we calculate all the terms appearing in $T''(0)$ in (3.52).

i). Calculation of $T'_3(0)$ and $T''_3(0)$.

Applying Proposition 2.7 to system (3.47), we have

$$T'_3(0) = \exp \left(\int_{x_0}^{X_0} \frac{1+Bx}{x^2} dx \right) = \left(\frac{X_0}{x_0} \right)^B \exp \left(\frac{1}{x_0} - \frac{1}{X_0} \right) \quad (3.53)$$

and

$$\begin{aligned} \frac{T''_3(0)}{T'_3(0)} &= 2 \int_{x_0}^{X_0} \left(\frac{x}{x_0} \right)^B \exp \left(\frac{1}{x_0} - \frac{1}{x} \right) \frac{-(1+Bx)}{x^4} dx \\ &= -2x_0^{-B} e^{\frac{1}{x_0}} \int_{x_0}^{X_0} (Bx^{B-3} + x^{B-4}) e^{-\frac{1}{x}} dx. \end{aligned} \quad (3.54)$$

ii). Calculations at Q_2

The system located at Q_2 in $(u, z) = (\frac{y}{x}, \frac{1}{x})$ coordinates has the form

$$\begin{cases} \dot{u} &= (B-1)u + uz - u^2 z, \\ \dot{z} &= -z(1+uz). \end{cases} \quad (3.55)$$

To bring system (3.55) to normal form, we first divided the system by $1+uz$, then

$$\begin{cases} \dot{u} &= (B-1)u + uz - (B-1)u^2 z + O(|(u, z)|^4) \\ \dot{z} &= -z. \end{cases} \quad (3.56)$$

So the normalizing change of coordinates have the form

$$u = U - UZ - \frac{B}{B-2} U^2 Z + \frac{1}{2} U Z^2 + O(|(U, Z)|^4), \quad z = Z$$

yielding

$$U = u + uz + \frac{B}{B-2} u^2 z - \frac{1}{2} u z^2 + O(|(u, z)|^4), \quad Z = z.$$

So on $Z = Z_0$, the change of coordinate T_5 can be written as

$$T_5(u) = [1 + Z_0 + O(Z_0^2)]u + [\frac{B}{B-2} Z_0 + O(Z_0^2)]u^2 + O(u^3).$$

Then we have

$$b_1 = 1 + Z_0 + O(Z_0^2), \quad b_2 = \frac{B}{B-2} Z_0 + O(Z_0^2). \quad (3.57)$$

Hence

$$\frac{b_2}{b_1} = \frac{B}{B-2}Z_0 + O(Z_0^2). \quad (3.58)$$

Also $T_6 = \text{identity}$.

iii) Normal form at the origin Q_1

We diagonalize the normal form by means of $x_1 = x + y$. Then

$$\begin{cases} \dot{x}_1 &= x_1^2 + (2-B)x_1y + (1-B)y^2, \\ \dot{y} &= y + By^2 + Bx_1y. \end{cases} \quad (3.59)$$

We divide system (3.59) by $1 + Bx_1 + By$. One can verify that the normalizing change of coordinate of the form

$$X = x_1 - (2-B)x_1y - \frac{1-B}{2}y^2 + O(|(x_1, y)|^3), \quad Y = y \quad (3.60)$$

transforms system (3.59) into a normal form

$$\begin{cases} \dot{X} &= X^2, \\ \dot{Y} &= Y(1 + BX). \end{cases} \quad (3.61)$$

Hence in the new coordinates, the section $x = x_0$ has the equation

$$X = h_1(Y) = x_0 + Y(-1 + O(x_0) + O(Y^2)). \quad (3.62)$$

In particular, $h(0) = x_0$, $h'_1(0) = -1$.

It follows from (3.61) that we have

$$\int_{x_0}^{h_1(Y)} \frac{1+Bx}{x^2} dx = \int_Y^{T_1(Y)} dY.$$

A straightforward calculation yields

$$T_1(y) = Y - \left(\frac{B}{x_0} + \frac{1}{x_0^2} \right) Y^2 + O(Y^3). \quad (3.63)$$

Hence

$$T'_1(0) = 1, \quad T''_1(0) = -2 \left(\frac{B}{x_0} + \frac{1}{x_0^2} \right). \quad (3.64)$$

As $Y = y$ we have

$$a_1 = 1, \quad a_2 = 0. \quad (3.65)$$

Let us take $Z_0 = x_0$ and $X_0 = \frac{1}{x_0}$ and let $x_0 > 0$ sufficiently small. Note that $1 < B < 2$, it follows from substitution of (3.51), (3.53), (3.54), (3.58), (3.64) and (3.65) into (3.52) and a straightforward calculation gives

$$\begin{aligned} T''(0) &= x_0^{1-2B} e^{\frac{1}{x_0}} (1 + O(x_0)) \left[-2 \left(\frac{B}{x_0} + \frac{1}{x_0^2} \right) \right. \\ &\quad \left. - 2x_0^{-B} e^{\frac{1}{x_0}} \int_{x_0}^{\frac{1}{x_0}} (Bx^{B-3} + x^{B-4}) e^{-\frac{1}{x}} dx + 2x_0^{2-2B} e^{\frac{1}{x_0}} \left(\frac{B}{B-2} + O(x_0) \right) \right] \\ &= x_0^{1-3B} e^{\frac{2}{x_0}} \left[-2 \int_{x_0}^{\frac{1}{x_0}} (Bx^{B-3} + x^{B-4}) e^{-\frac{1}{x}} dx + O(x_0^{2-B}) \right] \\ &< 0. \end{aligned} \quad (3.66)$$

where since $1 < B < 2$, we have $0 < 2-B < 1$ and $-2 < B-3 < -1$. \square

3.6 Finite cyclicity of (I_{17a}^2) and (I_{18a}^2)

Theorem 3.16. *The graphics (I_{17a}^2) and (I_{18a}^2) have finite cyclicity.*

Proof. Let us consider (I_{17a}^2) and the sections as defined in Fig. 15.

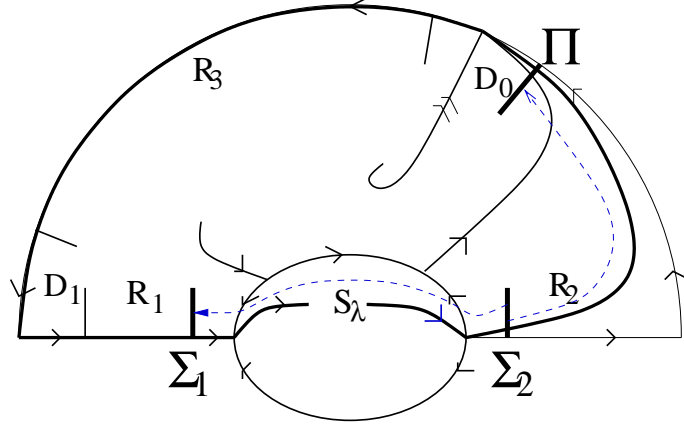


Figure 18: The transition maps for (I_{17a}^2)

We consider the displacement map $V : \Sigma_2 \longrightarrow \Sigma_1$ given by $V_\lambda(y) = R_\lambda(y) - S_\lambda(y)$ as in Theorem. 3.12. As before we write the proof in the case $a(0)$ irrational. For the passage near the saddle-node at infinity we can suppose that the normal form is taken so that the equator coincides with one coordinate axis. Then we can scale the normalizing coordinates so that the graphic cuts a section Π transversal to the equator at a height 1 (Fig.18). The transition $R_{2,\lambda}(y) : \Sigma_2 \longrightarrow \Pi$ can be taken as

$$R_{2,\lambda}(y) = 1 + T_{1,\lambda}(y)$$

where $T_{1,0}(0) = 0$ and $T'_{1,\lambda}(0) > 0$.

We can choose the normalizing coordinates so that R_3 is a linear map. Then the displacement map has the form

$$V_\lambda(y) = R_{1,\lambda} \left((m_1(\lambda)(1 + T_{1,\lambda}(y)))^{\frac{1}{\sigma(\lambda)}} \right) - S_\lambda(y). \quad (3.67)$$

Let

$$\tilde{y} = m_1(\lambda) \left(1 + T_{1,\lambda}(y) \right)^{\frac{1}{\sigma(\lambda)}}.$$

Then

$$V'_\lambda(y) = R'_{1,\lambda}(\tilde{y}) m_1(\lambda)^{\frac{1}{\sigma(\lambda)}} \left(1 + T_{1,\lambda}(y) \right)^{\frac{1}{\sigma(\lambda)} - 1} T'_{1,\lambda}(y) - S'_\lambda(y). \quad (3.68)$$

For limit periodic sets of type Epp1 (resp. Epp3) $V'_\lambda(y)$ is nonzero (resp. large) yielding cyclicity ≤ 1 as $\sigma(\lambda) < 1$.

For limit periodic set of type Epp2 we have $S'_\lambda(y) = *m_2(\lambda)(1 + O(\nu^{\sigma_1})O(y))$, where $*$ is a nonzero constant. Let

$$W_\lambda(y) = \frac{V'_\lambda(y)}{(m_1(\lambda))^{\frac{1}{\sigma(\lambda)}} (1 + O(\nu^{\sigma_1})O(y))}. \quad (3.69)$$

Then

$$\begin{aligned}
W'(y) = & R''_{1,\lambda}(\tilde{y})m_1(\lambda)^{\frac{1}{\sigma(\lambda)}}(1 + T_{1,\lambda}(y))^{2(\frac{1}{\sigma(\lambda)}-1)}T'_{1,\lambda}{}^2(y) \\
& + \frac{1-\sigma(\lambda)}{\sigma(\lambda)}R'_{1,\lambda}(\tilde{y})(1 + T_{1,\lambda}(y))^{\frac{1}{\sigma(\lambda)}-2}T'_{1,\lambda}{}^2(y) \\
& + R'_{1,\lambda}(\tilde{y})(1 + T_{1,\lambda}(y))^{\frac{1}{\sigma(\lambda)}-1}T''_{1,\lambda}(y) \\
& + O(\nu^{\sigma_1}).
\end{aligned}$$

The first and fourth terms are small as well as all their derivatives. Let us look at the sum of the second and third terms. It is given by a nonzero function multiplied by:

$$K_\lambda(y) = \frac{1 - \sigma(\lambda)}{\sigma(\lambda)}(T'_{1,\lambda})^2(y) + (1 + T_{1,\lambda}(y))T''_{1,\lambda}(y). \quad (3.70)$$

For $\lambda = 0$ the equation $K_0(y) \equiv 0$ can be integrated by quadratures. It is equivalent to say that $(1 + T_{1,0}(y))^{\frac{1}{\sigma(\lambda)}}$ is an affine map. Hence the proposition follows by finding a nonzero derivative of $W'(y)$ as soon as we show that $K_0(y)$ has a nonlinear term, which is equivalent to say that, at a finite order $(1 + T_{1,0}(y))^{\frac{1}{\sigma(\lambda)}}$ differs from an affine map.

We can choose analytic coordinates on Σ_2 and Π . By the analytic extension principle it suffices to verify the condition for graphics very close to the semicycle. There the transition map is the composition of a regular map together with a Dulac map for which $\sigma < 1$ and a regular map with non-vanishing second derivative. This last property is exactly the needed obstruction which guarantees that $(1 + T_{1,0}(0))^{\frac{1}{\sigma(0)}}$ differs from an affine map.

Proving that the graphic (I_{18a}^2) has finite cyclicity is completely similar. \square

References

- [1] F. Dumortier, M. El. Morsalani and C. Rousseau, *Hilbert's 16th problem for quadratic systems and cyclicity of elementary graphics*. Nonlinearity 9 (1996), no. 5, 1209–1261.
- [2] F. Dumortier, A. Guzmán and C. Rousseau *Finite cyclicity of elementary graphics surrounding a focus or center in quadratic systems*, to appear in Qualitative Theory of Dynamical Systems.
- [3] F. Dumortier, Y. Ilyashenko and C. Rousseau, *Normal forms near a saddle-node and applications to finite cyclicity of graphics*, Erg. Th. Dynam. Syst. 22 (2002), 783–818.
- [4] F. Dumortier, R. Roussarie and C. Rousseau, *Hilbert's 16th problem for quadratic vector fields*. J. Differential Equations 110 (1994), no. 1, 86–133.
- [5] F. Dumortier, R. Roussarie and C. Rousseau, *Elementary graphics of cyclicity 1 and 2*. Nonlinearity 7 (1994), no. 3, 1001–1043.
- [6] F. Dumortier, R. Roussarie and S. Sotomayor, *Generic 3-parameter families of vector fields in the plane, unfoldings of saddle, focus and elliptic singularities with nilpotent linear parts*. Springer Lecture Notes in Mathematics 1480 1-164 (1991).
- [7] F. Dumortier, R. Roussarie and S. Sotomayor, *Bifurcations of Cuspidal Loops*. Nonlinearity 10 (1997), no. 6, 1369–1408.

- [8] M. El Morsalani, *Perturbations of graphics with semi-hyperbolic singularities*, Bull. Sciences Mathématiques, Vol. 120, (1996), 337–366.
- [9] A. Guzmán and C. Rousseau, *Genericity conditions for finite cyclicity of elementary graphics*. J. Differential Equations 155 (1999), no. 1, 44–72.
- [10] Y. Ilyashenko and S. Yakovenko, *Finite-smooth normal forms of local families of diffeomorphisms and vector fields*. Russian Math. Surveys 46, (1991), 1–43.
- [11] A. Kotova and V. Stanzo, *On few-parameter generic families of vector fields on the two-dimensional sphere*. Concerning the Hilbert 16th problem. 155–201, Amer. Math. Soc. Transl. Ser. 2, 165, Amer. Math. Soc., Providence, RI, 1995.
- [12] A. Mourtada, *Cyclicité finie des polycycles hyperboliques de champs de vecteurs du plan: mise sous forme normale*. Bifurcations of planar vector fields (Luminy, 1989), 272–314, Lecture Notes in Math., 1455, Springer, Berlin, 1990.
- [13] S. Sternberg, *On the structure of local homeomorphisms of euclidean n -space. II*. Amer. J. Math. 80, (1958), 623–631.
- [14] F. Takens, *Singularities of vector fields*. Publ. Math. de l’IHES 43, 47–100, 1974.
- [15] H. Zhu and C. Rousseau *Finite cyclicity of graphics with a nilpotent singularity of saddle or elliptic type*, J. Differential Equations, Vol. 178, No.2, 325–436. (2002)